

# Space Weather



## REVIEW ARTICLE

10.1029/2020SW002593

### Key Points:

- Reasonable worst-case scenarios have been developed to support assessment of severe space weather within the UK National Risk Assessment
- Individual scenarios focus on space weather features that disrupt a particular national infrastructure, e.g. electric power or satellites
- Treat these scenarios as an ensemble, enabling planning for a severe space weather event within which many of these features will arise

### Supporting Information:

- Supporting Information S1

### Correspondence to:

M. Hapgood,  
[mike.hapgood@stfc.ac.uk](mailto:mike.hapgood@stfc.ac.uk)

### Citation:

Hapgood, M., Angling, M. J., Attrill, G., Bisi, M., Cannon, P. S., Dyer, C., et al. (2021). Development of space weather reasonable worst-case scenarios for the UK National Risk Assessment. *Space Weather*, 19, e2020SW002593. <https://doi.org/10.1029/2020SW002593>

Received 19 JUL 2020

Accepted 27 JAN 2021

## Development of Space Weather Reasonable Worst-Case Scenarios for the UK National Risk Assessment

Mike Hapgood<sup>1</sup> , Matthew J. Angling<sup>2</sup> , Gemma Attrill<sup>3</sup>, Mario Bisi<sup>1</sup> , Paul S. Cannon<sup>4</sup> , Clive Dyer<sup>5,6</sup> , Jonathan P. Eastwood<sup>7</sup> , Sean Elvidge<sup>4</sup> , Mark Gibbs<sup>8</sup> , Richard A. Harrison<sup>1</sup> , Colin Hord<sup>9</sup>, Richard B. Horne<sup>10</sup> , David R. Jackson<sup>8</sup> , Bryn Jones<sup>11</sup>, Simon Machin<sup>8</sup> , Cathryn N. Mitchell<sup>12</sup>, John Preston<sup>13</sup> , John Rees<sup>14</sup>, Neil C. Rogers<sup>15</sup> , Graham Routledge<sup>16</sup> , Keith Ryden<sup>5</sup> , Rick Tanner<sup>17</sup>, Alan W. P. Thomson<sup>18</sup> , James A. Wild<sup>15</sup> , and Mike Willis<sup>19</sup>

<sup>1</sup>RAL Space, STFC Rutherford Appleton Laboratory, Harwell Campus, Didcot, Oxfordshire, UK, <sup>2</sup>Spire, Unit 5A, Glasgow, UK, <sup>3</sup>Defence Science and Technology Laboratory, Intelligence Innovation, RAF Wyton, Huntingdon, UK, <sup>4</sup>School of Engineering, University of Birmingham, Edgbaston, Birmingham, UK, <sup>5</sup>Department of Electrical and Electronic Engineering, Surrey Space Centre, University of Surrey, Guildford Surrey, UK, <sup>6</sup>CSDRadConsultancy Ltd, Fleet, UK, <sup>7</sup>Imperial College, Space and Atmospheric Physics, The Blackett Laboratory, Imperial College London, London, UK, <sup>8</sup>Met Office, Exeter, Devon, UK, <sup>9</sup>Civil Aviation Authority, Aviation House, Crawley, West Sussex, UK, <sup>10</sup>British Antarctic Survey, Cambridge, UK, <sup>11</sup>SolarMetrics Ltd., Swindon, UK, <sup>12</sup>Centre for Space, Atmospheric and Oceanic Science, University of Bath, Claverton Down, Bath, UK, <sup>13</sup>Department of Sociology, University of Essex, Wivenhoe Park, Colchester, UK, <sup>14</sup>British Geological Survey, Environmental Science Centre, Nicker Hill, Keyworth, Nottingham, UK, <sup>15</sup>Department of Physics, Lancaster University, Lancaster, UK, <sup>16</sup>Defence Science and Technology Laboratory, Portsmouth West, Fareham, UK, <sup>17</sup>PHE Centre for Radiation, Chemical and Environmental Hazards, Harwell Campus, Didcot, Oxfordshire, UK, <sup>18</sup>British Geological Survey, The Lyell Centre, Research Avenue South, Edinburgh, UK, <sup>19</sup>UK Space Agency, Polaris House, Swindon, UK

**Abstract** Severe space weather was identified as a risk to the UK in 2010 as part of a wider review of natural hazards triggered by the societal disruption caused by the eruption of the Eyjafjallajökull volcano in April of that year. To support further risk assessment by government officials, and at their request, we developed a set of reasonable worst-case scenarios and first published them as a technical report in 2012 (current version published in 2020). Each scenario focused on a space weather environment that could disrupt a particular national infrastructure such as electric power or satellites, thus, enabling officials to explore the resilience of that infrastructure against severe space weather through discussions with relevant experts from other parts of government and with the operators of that infrastructure. This approach also encouraged us to focus on the environmental features that are key to generating adverse impacts. In this paper, we outline the scientific evidence that we have used to develop these scenarios, and the refinements made to them as new evidence emerged. We show how these scenarios are also considered as an ensemble so that government officials can prepare for a severe space weather event, during which many or all of the different scenarios will materialize. Finally, we note that this ensemble also needs to include insights into how public behavior will play out during a severe space weather event and hence the importance of providing robust, evidence-based information on space weather and its adverse impacts.

**Plain Language Summary** Severe space weather was identified as a risk to the UK in 2010 as part of a wider review of natural hazards following the societal disruption that arose when airspace was closed in April 2010 due to volcanic ash. To support further risk assessment by government officials, we developed a set of scenarios, each focused on how severe space weather conditions could disrupt a particular national infrastructure, e.g. the impact of large rapid geomagnetic field changes on the power grid. These scenarios enabled officials to discuss infrastructure resilience against space weather with relevant experts in government and industry. In this paper, we outline the scientific evidence that we have used to develop these scenarios, and the refinements made to them as new evidence emerged. We also show how these scenarios may occur close together in time so that government officials must prepare for the near-simultaneous occurrence of many different problems during a severe space weather event, including the need to consider how public behavior will play out during a severe space weather event. This highlights the importance of providing robust, evidence-based information on space weather and its adverse impacts.

© 2021. The Authors.

This is an open access article under the terms of the [Creative Commons Attribution License](https://creativecommons.org/licenses/by/4.0/), which permits use, distribution and reproduction in any medium, provided the original work is properly cited.

## 1. Introduction

The past decade has seen increased awareness of the need for societal resilience against the full range of natural hazards that can seriously disrupt everyday life. A key trigger for this was the 2010 eruption of Eyjafjallajökull. The ash clouds from this Icelandic volcano drifted over much of Northern Europe, triggering a shutdown of air space for several days, leading to widespread disruption of air transport, overloading of ground transport, and economic disruption within and beyond Europe (Oxford Economics, 2010). Within the UK, the subsequent reviews quickly identified that these adverse impacts would have been much less if pre-existing scientific knowledge had been factored into the National Risk Assessment process (some background on this process is provided in the Supplementary Information, together with a summary of non-malicious risks considered in the Assessment, including space weather and pandemic disease). Those reviews also opened up a key question: were there any other unassessed natural hazards for which there is credible scientific evidence of potential to cause severe societal and economic disruption? This quickly identified space weather (disturbances of the upper atmosphere and near-space environment that can disrupt technology) as an important issue for the UK National Risk Assessment process (Cabinet Office, 2012) and initiated the development of a set of “reasonable worst-case scenario” (RWCSs) for use in the assessment process. To facilitate that development an independent expert group, the Space Environment Impacts Expert Group (SEIEG) was set up in the autumn of 2010 and has also provided support for related activities such as exercises to explore how to manage severe space weather events. This paper provides scientific background to the work undertaken by SEIEG to develop the risk scenarios.

### 1.1. Background: Delivering the RWCS to Government

The RWCS has been an evolving series of technical reports with three versions formally published since this work started in 2010 (Hapgood et al., 2012, 2016, 2020). All are openly available on-line, and structured to address the needs of government officials. Those officials need concise information on the severe space weather conditions that may disrupt critical national infrastructures (Cabinet Office, 2019). These infrastructures include the power grid, transport (aviation, rail), and satellite applications such as Global Navigation Satellite Systems (GNSS) and communications. They also include generic capabilities such as the electronic control systems that are now ubiquitous in everyday life, not least in the critical infrastructures that sustain that life. As a result, each of the technical reports provides a set of RWCSs, each summarizing the severe space weather conditions relevant to a particular aspect of critical infrastructures. Most importantly, we identify which environmental parameters are crucial to the adverse impacts of space weather on a particular infrastructure, given our appreciation of how space weather impacts engineered systems (e.g. see P. Cannon et al., 2013), and also of the potential societal impacts (e.g. Sciencewise, 2015). Thus each infrastructure-specific RWCS provides a concise summary of:

- a rationale for the choice of each environmental parameter, including a summary of anticipated effects on systems at risk from severe values of that parameter
- our assessment of the reasonable worst case values for that parameter, typically conditions that may occur about once per century, a benchmark that is widely used in risk assessment by governments (M. Hapgood, 2018). But rarer events are considered where they may lead to catastrophic impacts, e.g. risks to the operation of nuclear power systems (HSE, 1992)
- the spatial and temporal scales over which severe conditions are thought to manifest
- the provenance of information on severe conditions, with priority given to sources in the peer-reviewed literature
- our assessment of the quality of this information, and where more work may improve that quality. We emphasize that each RWCS is an interpretation of existing scientific literature, and is open to revision as additional scientific knowledge becomes available

This RWCS format was developed in consultation with officials from the UK Government’s Civil Contingencies Secretariat. It gives our government colleagues a concise document that they can use when engaging with public and private sector organizations that operate critical infrastructures affected by space weather. As we note above, the latest RWCS report is openly available on-line and we encourage readers to use that as the primary source. To assist readers, we provide cross-references to key RWCS sections at appropriate

points in later sections of this paper. We do not repeat or summarize the RWCS here as it is important that we avoid creating a secondary source.

## 1.2. Purpose of This Paper

The aim of the present paper is to provide the space weather community with insights into how we developed the technical content of the most recent RWCS reports, though there is significant overlap with the two previous RWCS reports since this development is an evolutionary process that responds to advances in scientific understanding. One major example over the period since the first RWCS report has been the growing set of evidence on historical radiation storms, notably the 774/5 AD event first reported by Miyake et al (2012). Subsequent papers including Mekhaldi et al. (2015), C. Dyer et al. (2017), O'Hare et al. (2019), and Miyake et al. (2020) have expanded our understanding of these extreme events and their implications for the RWCSs on systems affected by space and atmospheric radiation environments.

In the rest of this paper, we first present the details behind the infrastructure-specific RWCSs, and then explore how the individual RWCSs may arise in parallel during a severe space weather event. This parallelism has been an important consideration for us as a severe space weather event will cause problems in different economic sectors close together in time. It is one of the factors that drives the ranking of space weather as a significant risk in the UK National Risk Register. Thus our work has to capture both the detail (which is important for dealing with specific economic sectors) and the potential for diverse problems to occur close together in time.

We group the details into a series of sections. Section 2 discusses the RWCSs for electrically grounded systems, including electricity transmission networks, pipelines and railway. Section 3 discusses those for ionospheric space weather effects on a wide range of radio applications including GNSS, high-frequency (HF) radio communications, satellite communications over a range of frequencies (e.g. VHF, UHF, and L-band). Section 4 discusses the RWCSs for satellite operations including the effects of particle radiation, electrical charging and atmospheric drag, and outlines the potential impacts on satellite launches, a topic that is becoming important as the UK develops its own launch capabilities. Section 5 discusses the RWCSs for atmospheric radiation effects on aviation, and on terrestrial electronics. Section 6 outlines how solar radio bursts can impact radio technologies including GNSS and radars. The organization of these sections reflects our way of working, which emerged from the interplay between science, engineering and the need to consider impacts on specific infrastructures. For example, it is natural to group together all impacts that affect satellite operations since that sector is well-structured to handle risks at both design and operations levels. In contrast, the ionospheric effects on radio systems are grouped across infrastructure sectors since the engineering study of radio signal propagation works across sectors. In other cases, there is a natural focus around a physical effect that impacts multiple infrastructures (e.g. electrically grounded systems). This diverse approach has proved effective in establishing the details of the different RWCSs, allowing us to address each area of focus as best suits that area; this is reflected in differences of structure within Sections 2 to 6.

The potential for many different space weather effects to occur close together in time is addressed in Section 7, where we outline how two terrestrial manifestations of space weather each drive a diverse set of RWCSs. Geomagnetic storms contribute to RWCSs for power grids, rail systems, GNSS, HF radio, satellite drag, and charging, while radiation storms contribute to RWCSs for satellite operations, aviation, ground systems, and HF radio. We discuss how these two types of storms generate links between RWCSs, links that need to be appreciated by policy makers and system operators as they cause seemingly different problems to arise simultaneously. This then leads into Section 8, where we widen our set of scenarios to discuss the possible effects of severe space weather on public behavior, taking account of the links between RWCSs. In the final section, we review the current state of knowledge concerning severe space weather environments; we identify key areas for improvement, and discuss how these may be addressed.

## 1.3. Key Drivers of Space Weather

The focus of this paper is on the space weather environments that most immediately impact the operation of critical infrastructures. As we will discuss below those impacts can take several forms including:

(a) interactions with hardware and software systems, (b) delay, distortion and absorption of radio signals during propagation, and (c) human radiation exposure. Thus, we focus mainly on the terrestrial end of the chain of physics by which the Sun generates space weather phenomena at Earth. But, when needed, we do discuss key solar and heliospheric phenomena. These include coronal mass ejections (CMEs), high-speed streams (HSSs), and stream interaction regions (SIRs), as solar wind features that drive geomagnetic activity (both storms and substorms) and radiation belt activity (especially enhanced fluxes of high-energy electrons), (b) solar flares, as the causes of dayside radio blackouts, and (c) solar energetic particles (SEPs) which may be energized in a solar flare reconnection event or a CME-driven shock near the Sun. Solar energetic particle (SEP) events have a direct impact on the Earth and near-Earth environment as they have an immediate impact on satellite operations, as well being the driver of atmospheric radiation storms. Similarly, we directly consider solar radio bursts as they have an immediate effect on some radio receiver systems.

Geomagnetic activity arises when CMEs and SIRs arrive at Earth. If these are preceded by a shock, their arrival can produce a rapid compression of the magnetosphere, which is observed on ground as a sharp increase in the strength of the magnetic field, typically by a few tens of nT, known as a sudden impulse. If followed by a geomagnetic storm, it is also termed a sudden storm commencement. If the CMEs and SIRs contain a southward magnetic field (opposite to the northward field in Earth's magnetosphere) solar wind energy and momentum can flow into Earth's magnetosphere, via magnetic reconnection. This inflow can drive a circulation of plasma and magnetic flux with the magnetosphere, known as the Dungey cycle, in which energy is temporarily stored in the tail of the magnetosphere and then released in bursts that we term substorms. These can produce bursts of electric currents in the ionosphere at high, and sometimes mid, latitudes, and injections of charged particles into the ring current, the torus of electric current that encircles the Earth around 10,000–20,000 km above the equator. Changes in these currents manifest on the ground as variations in the surface geomagnetic field, and are a key driver of the geomagnetically induced currents discussed in Section 2. If CMEs and SIRs can drive an extended period of geomagnetic activity, often with examples of all these geomagnetic phenomena, it is termed a geomagnetic storm and is typically characterized by the build-up of the ring current to high levels.

Geomagnetic activity also has profound and complex impacts on the upper atmosphere, both the thermosphere and the ionosphere. For example, the heating of the polar thermosphere during geomagnetic activity drives changes in global pattern of thermospheric winds, and also an uplift of denser material from the lower thermosphere – leading to changes in composition and density of the thermosphere, which affect satellite operations as discussed in more detail in Section 4.2. These changes in the thermosphere drive further changes in density of the ionosphere, for example by changing the rate at which ionization is lost by dissociative recombination. These storm effects in the ionosphere, and their impacts on radio systems, are discussed in more detail in Sections 3.1, 3.2, 3.3, and 3.4.2. The ionosphere is also affected by SEPs and solar flares. Both can produce ionization at altitudes below 90 km, leading to the absorption of HF and VHF radio waves as discussed in Section 3.4.1; high energy electron precipitation during geomagnetic activity also contributes to this low altitude ionization, and the associated radio wave absorption.

SEPs also have significant impacts on satellites. As discussed in Section 4.1, charged particles at energies above 1 MeV can penetrate into satellite systems, causing radiation damage (the displacement of nuclei within the material structure of those systems) and single event effects (SEEs). The latter arise from the generation of ionization within electronic devices leading to a range of adverse effects including the flipping of computer bits in memory (single event upsets), and the generation of electron cascades that damage parts or all of those devices (single gate rupture and burnout); see Box 2 of P. Cannon et al. (2013) for an overview of the wider range of SEEs. SEPs can also penetrate deep into Earth's atmosphere where they collide with atmospheric species to produce enhanced levels of radiation in the form of neutrons and muons. The enhanced atmospheric radiation can have adverse impacts on electronic systems and human health as discussed in Section 5.

Finally, we note that our remit is to address space weather as a natural hazard (and hence as a “non-malicious risk” within the UK National Risk Assessment). We do not address anthropogenic processes that can generate space weather effects (Gombosi et al., 2017), but do note where such effects (e.g. artificial radiation belts) provide helpful insights for our understanding of naturally occurring space weather.

#### 1.4. Notes on Nomenclature

To ensure consistency across the wide range of space weather events and data presented in this paper, we have adopted the following conventions:

- The Carrington event of 1859. We recognize that this severe space weather event is sometimes called the Carrington-Hodgson event to reflect that the initial flare was observed simultaneously by two respected observers in different parts of London (Carrington, 1859; Hodgson, 1859). For simplicity, we refer to it as the Carrington event in the rest of this paper
- We sometimes use the older term co-rotating interaction region (CIR) alongside the modern term stream interaction region. A CIR is a special case in which an SIR persists for more than a synodic solar rotation period of 27 days, and hence will impact Earth repeatedly at 27-day intervals, perhaps for several months. We use the two terms here to recognize that both are still widely used in the expert community
- Particle fluxes are presented in areal units of  $\text{cm}^{-2}$  rather than  $\text{m}^{-2}$ , as would follow from a strict application of SI units. We do this to recognize that most radiation experts are more used to using  $\text{cm}^{-2}$
- Aircraft flight altitudes are presented in units of feet in line with international aviation practice; we also provide kilometers in parentheses, when a value in feet is first presented

## 2. Geomagnetically Induced Currents

Here we discuss impacts of GIC on electricity transmission, pipeline, and rail networks. This underpins a number of RWCSs as discussed in M. Hapgood et al. (2020): Section 7.1 for power grids and Section 7.14 for railway signal systems. It is not currently clear if we need RWCSs for pipelines and railway electric traction systems.

### 2.1. Introduction

Rapid, high-amplitude magnetic variations during magnetic storms induce a geoelectric field,  $E$ , in the conducting Earth, and in conductors at the Earth's surface. This  $E$ -field causes electrical currents – Geomagnetically Induced Currents (GIC) – to flow in conducting structures grounded in the Earth (e.g. Boteler, 2014). GICs are therefore a potential hazard to industrial networks, such as railways, metal oil, and gas pipelines, and high-voltage electrical power grids, during severe space weather.

The GIC hazard can be assessed using the time rate of change of the vector magnetic field in the horizontal plane ( $dB_H/dt$ ) or the induced  $E$ -field as the key parameter. In the UK,  $E$ -fields are spatially complex, due to the conductivity and structure of the underlying geology, and of the surrounding seas (e.g. Beggan et al., 2013). High values of  $dB_H/dt$  generally occur as short bursts due to rapid changes in ionospheric and magnetospheric current systems, and are most common during geomagnetic storms due to phenomena such as substorms, sudden commencements, or particle injections into the ring current. The largest recorded disturbance of the last 40 years in Europe, in terms of  $dB_H/dt$ , was 2,700  $\text{nT min}^{-1}$ , measured in southern Sweden in July 1982 (Kappenman, 2006), while the largest UK  $dB_H/dt$  was 1,100  $\text{nT min}^{-1}$  in March 1989 (e.g. as shown in Figure 6 of A. W. P. Thomson et al., 2011, see also in the supporting information), both during substorms. Extreme value statistical studies (Rogers et al., 2020; A. W. P. Thomson et al., 2011) suggest that, for the UK, the largest  $dB_H/dt$  is of the order of several thousand  $\text{nT min}^{-1}$ . Taking the worst-case as the upper limit of the 95% confidence interval on the predicted extreme values, these studies suggest that the worst-case  $dB_H/dt$  in one hundred years is 4,000–5,000  $\text{nT min}^{-1}$  (rising to 8,000–9,000  $\text{nT min}^{-1}$  for the two-hundred year worst case). However, there remains considerable uncertainty in these estimates and further research is required, e.g. to fully understand the occurrence of large, but short-lived, excursions in  $dB_H/dt$ , such as in the 1982 and 1989 observations above, also examples reported during the severe storms in May 1921 (Stenquist, 1925) and October 2003 (Cid et al., 2015). Local peak electric fields of  $\sim 20$ – $25$  V/km have been estimated for the largest events such as the Carrington Storm of 1859 (e.g. Beggan et al., 2013; Kelly et al., 2017; Ngwira et al., 2013; Pulkkinen et al., 2015). These intense events may have spatial scales of several hundred km (Ngwira et al., 2015; Pulkkinen et al., 2015). Thus, a single event, essentially a 1–2 min duration “spike” in  $dB_H/dt$  or  $E$  during a magnetic storm, could simultaneously cover a sizeable fraction of the UK landmass.

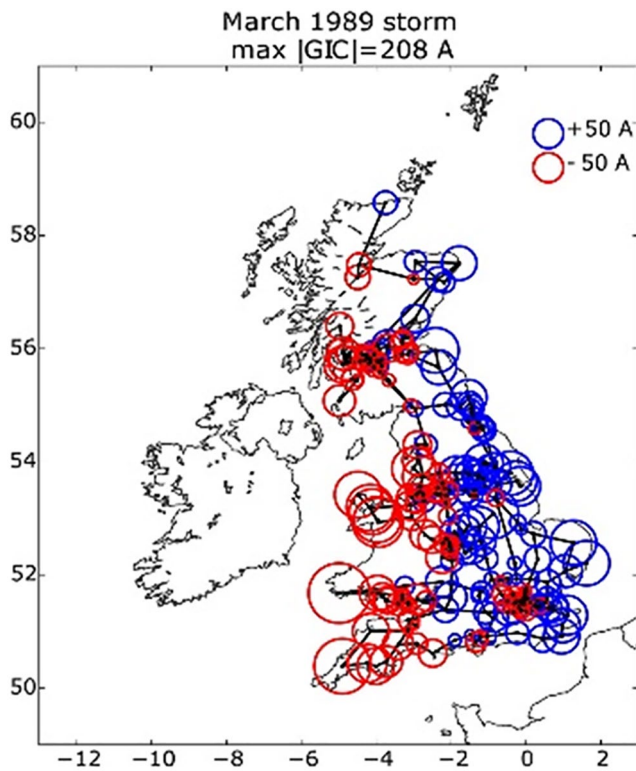


**Figure 1.** The maximum GIC experienced at each node/substation in the UK transmission system at any time during the March 1989 magnetic storm, according to the model of Kelly et al. (2017).

The probability of occurrence of these intense localized disturbances is largely determined by the frequency of severe geomagnetic storms, as such storms can produce multiple bursts of large  $dB_H/dt$  at different times and longitudes, as occurred during the 1989 storm (Boteler, 2019), and even repeated large bursts a day or more apart at the same location as occurred in Sweden during the May 1921 storm (M. Hapgood, 2019a). The likelihood of repeated intense events at any particular location over a few days is a significant hazard during the most severe storms (see Table IV of Oughton et al, 2019).

The overall magnitude of severe storms is characterized by large negative values of the hourly disturbance storm time,  $Dst$ , magnetic activity index. But this is a measure of the total intensity of the ring current, not of  $dB_H/dt$ . The ring current builds up during intense magnetic activity, but decays only slowly, often producing the largest negative value of  $Dst$  some hours after bursts of large  $dB_H/dt$ , e.g. the 1989 UK large  $dB_H/dt$  disturbance above occurred around 4 h before minimum  $Dst$ . Thus, we focus here on  $Dst$  as a tool to assess the frequency of severe geomagnetic storms. Examples of such storms include the Carrington event and the May 1921 storms for which recent estimates of minimum  $Dst$  are around  $-900$  nT (Cliver & Dietrich, 2013; Love et al, 2019); the spectacular storm of September 1770 (Hayakawa et al., 2017; Kataoka & Iwahashi, 2017) is probably also in this category. The recurrence likelihood of such storms has been the subject of several studies (Chapman et al., 2020; Elvidge, 2020; Jonas et al., 2018; Love, 2012; Riley, 2012; Riley & Love, 2017), all which suggest that we should expect to experience such severe storms on centennial timescales.

$E$ -field and of  $dB_H/dt$ , together with better models of ground conductivity and the flow of GIC in conducting networks (e.g. Pulkkinen et al., 2017).

To further improve the certainty of what may be considered a *reasonable* worst-case scenario and its impacts, we require independently derived estimates of extremes, in both amplitude and in space/time profile, of the

## 2.2. Electrical Transmission and Pipeline Networks

The consequences of severe space weather for the power transmission system include: tripping of safety systems potentially leading to regional outages or cascade failure of the grid; transmission system voltage instability and voltage sag; premature ageing of transformers leading to decreased capacity in months/years following an event (Gaunt, 2014); and physical damage, e.g. insulation burning, through transformer magnetic flux leakage. According to the executive summary of the report by P. Cannon et al. (2013), in response to a 1 in 100–200 year reasonable worst-case event of  $5,000$  nT  $\text{min}^{-1}$ , “... around six super grid transformers in England and Wales and a further seven grid transformers in Scotland could be damaged ... and taken out of service. The time to repair would be between weeks and months. In addition, current estimates indicate a potential for some local electricity interruptions of a few hours. ... National Grid’s analysis is that around two nodes in Great Britain could experience disconnection.” The report later notes that there are over 600 nodes in Great Britain, so the loss of power for an extended period would be limited to a few areas, but would be a severe emergency in those areas. Historical occurrences of  $dB_H/dt > \sim 500$  nT  $\text{min}^{-1}$  have been associated with enhanced risk to the UK grid (e.g. as documented in Erinmez et al., 2002). Modeled GIC for a  $5,000$  nT  $\text{min}^{-1}$   $dB_H/dt$ , suggest a per-substation GIC of hundreds of Amps, depending on substation and electrojet locations (Beggan et al., 2013; Kelly et al., 2017). Figure 1 shows modeled maxima GIC across the UK for the less severe 1989 storm, according to Kelly et al. (2017).

GICs induced by space weather can interfere with the operation of cathodic protection systems on pipeline networks, disrupting the control of those systems and leading to enhanced corrosion rates (Gummow, 2002; Ingham & Rodger, 2018). This impact arises where the induced pipe-to-soil potential (PSP), associated with

GICs and induced by the  $E$ -field, lies outside the normal operational limits (of order  $-1V$  with respect to Earth) of cathodic protection systems (e.g. Boteler, 2000). To date, in the UK, there has been no (or no publicly available) assessment of the space weather hazard to the high-pressure gas transmission system, though interference with cathodic protection systems in Scotland was noted during the March 1989 storm (Hapgood, private communication). However, Boteler (2013) describes measured and modeled PSP data for North American pipelines, demonstrating that tens of volts of PSP are feasible for  $E$ -fields of order  $1 V/km$ , particularly at pipe ends and at electrically insulated pipe junctions, in pipes of several hundred km extent. A. W. P. Thomson et al. (2005) estimated that peak UK  $E$ -fields reached  $\sim 5 V/km$  during the October 2003 storm, which suggests that UK pipelines, like those in North America, are likely to experience anomalous levels of PSP during severe events.

### 2.3. Rail Networks

Railway infrastructure and operations can be affected by induced electrical currents during severe space weather (e.g. Krausmann et al., 2015). Studies of railway operations at magnetic latitudes above  $50^\circ$  (Eroshenko et al., 2010; Wik et al., 2009) have shown that induced and/or stray currents from the ground during strong magnetic storms result in increased numbers of signaling anomalies. Although most such anomalies result in a *right-side failure*, i.e. a fail-safe situation in which signals incorrectly stop trains, a recent detailed analysis by Boteler (2020) shows that both *right-* and *wrong-side failures* are possible. In the latter case, signals incorrectly allow trains to enter an already occupied section of track, thus creating a collision risk. A space-weather impact study commissioned by the UK Department for Transport (Atkins, 2014) reports that induced direct current flowing in the overhead line equipment could cause a train's on-board transformer to overheat and shut down, while interference with on-board line current (fault) monitoring could also stop train movement. The extent to which track-staff workers are vulnerable to induced currents in cables and track is also unclear, suggesting that maintenance might need to be suspended during severe space weather. The UK railway network relies upon many modern technologies (including power, communications, and GNSS), so a set of complex interdependencies arise and introduce vulnerabilities beyond those associated with individual direct impacts on railway infrastructure. While power supply failures would severely degrade signaling operations, meanwhile, the unavailability of GNSS services would impact many non-safety critical railway systems, with the potential to lead to significant disruption. The study by Atkins (2014) notes that GSM-R ("Global System for Mobile Communications – Railway," now the primary communication system on UK railways), may be affected by solar radio bursts around sunrise and sunset (due to the directional antennas used by GSM-R), again leading to a loss of service and disruption to the network. Although these impacts are described here independently, the greatest uncertainty (and risk of disruption and safety issues) arises from the interconnectivity of these systems and from impacts arising from multiple, simultaneous space-weather effects. As noted by Atkins (2014), accidents are rarely caused by a single failure; compound effects from multiple impacts are more likely to create problems.

## 3. Ionospheric Impacts on Radio Systems

Here we discuss how radio signals propagating through the ionosphere are affected by space-weather-driven changes in the structure of the ionosphere. This underpins a number of RWCSs as discussed in M. Hapgood et al. (2020): Section 7.11 which discusses how ionospheric scintillation affects satcom, Sections 7.9 and 7.10 which discuss ionospheric effects on GNSS, and Sections 7.12 and 7.13 which discuss ionospheric effects on HF radio communications.

### 3.1. Background: Ionospheric Storms

The ionosphere varies on timescales ranging from seconds to years. Many of the diurnal and long-term variations are relatively cyclic and can be well-modeled climatologically. Space weather describes the irregular changes which are superimposed on this climatology. Large ionospheric space weather events are termed storms and are driven by solar and heliospheric phenomena as discussed in Section 1.3.

The spatial and temporal variations of the ionospheric electron density result in variations in both its local refractive index and the absorption of radio waves. In addition to large-scale variations are electron density

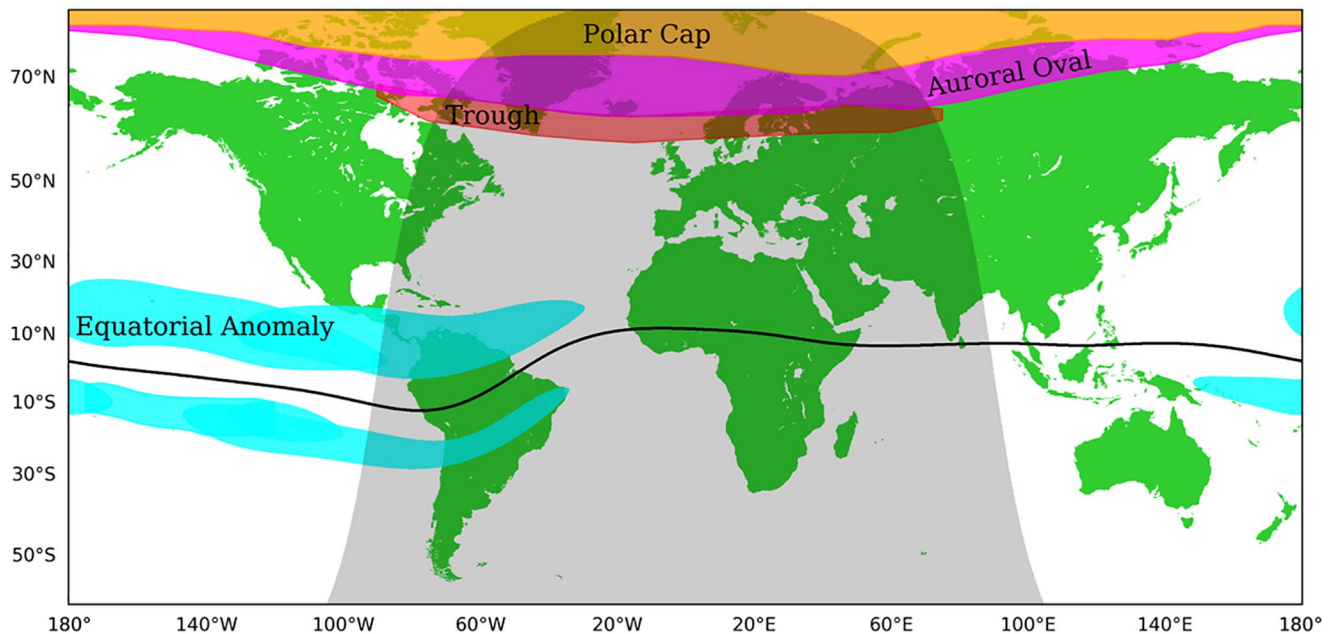


**Figure 2.** The main ionospheric regions during quiet conditions ( $F_{10.7} = 100$ ,  $K_p = 2$ ) at 00 UT on 1 September based on the equatorial anomaly description in NeQuick (Nava et al., 2008), the auroral oval model from Zhang and Paxton (2008) and the ionospheric trough model from Karpachev et al. (2016) and Aa et al. (2020).

irregularities ranging in size from meters to tens of kilometres. These diffract and scatter electromagnetic waves, with the small-scale irregularities causing amplitude and phase variations known as scintillation.

Ionospheric storm impacts show considerable geographic variations. We divide these into several regions as shown in Figure 2: the high-latitude region (including the polar cap, auroral zone and trough), the mid-latitude region, and the low-latitude region (including the equatorial anomalies).

In the high-latitude polar cap, ionospheric storms are associated with convection of patches of enhanced ionization from the dense dayside ionosphere to the less dense nightside ionosphere. These patches are associated with strong gradients and irregularities (Weber et al., 1984).

At auroral latitudes geomagnetic storms manifest as a series of substorms as energy is released from the tail of the magnetosphere. Enhanced particle precipitation into the D, E, and F-regions occurs and strong electric fields drive plasma instabilities. Together, these cause electron density gradients, irregularities, and new ionospheric layers in the night time E and F regions, and enhanced ionization in the D-region in both the midnight and morning sectors (see Section 3.4.1 for more detail). During large storms, the auroral ionosphere expands and shifts to lower latitudes. Observations of the visual aurora during the Carrington event indicates that the auroral ionosphere can expand to lower latitudes on multiple nights during a severe space weather event (Green & Boardsen, 2006).

Ionospheric storms at mid-latitudes often start with a positive phase of enhanced electron density lasting a few hours, associated with the sudden commencement signature of the geomagnetic storm. This is followed by a negative phase with decreased electron density, lasting several days associated with the geomagnetic main phase (e.g., Matsushita, 1959). During a severe event, it is possible that the usual mid-latitude phenomenology will be unrecognizable, with the high-latitude ionosphere moving to lower latitudes and the low-latitude ionosphere moving to higher latitudes, so that they are in relatively close proximity.

Considerable progress has been made in understanding low-latitude ionospheric storm processes in recent years, and it is widely recognized that thermospheric composition, neutral winds, and electrodynamic effects are all important. Notably, near the magnetic dip equator, ionospheric storms cause enhanced uplift of the ionization to high altitudes, which in turn causes electron density enhancements in the anomaly regions poleward of the magnetic equator (e.g., Basu et al., 2002; Mannucci et al., 2005). In the same regions,



Rayleigh-Taylor instabilities can generate small-scale electron density irregularities in the evening sector (P. M. Kintner et al., 2007). During very large storms, localized storm enhancements form at mid-latitudes and are uplifted to high altitudes on the dayside (Yin et al., 2006).

In the following sub-sections, the rationale for a range of reasonable worst-case ionospheric parameters are described by reference to the operating requirements of satellite communications, GNSS, and HF communications. In large part, these same ionospheric parameters also define the reasonable worst-case limitations of a number of other ionospheric radio systems, see for example, P. S. Cannon (2009).

### 3.2. Impacts on Satellite Communications

All communication systems are designed to tolerate variations in the signal amplitude and phase, but when signal fades are too severe and/or the phase too randomized (as in strong scintillation), message errors occur. Error correction codes and interleaving can mitigate these problems to some extent, but these fail if the channel variations are severe.

The effects of scintillation increase as the operating frequency is decreased and consequently, what is a major event at one frequency is minor at another. Even moderate ionospheric storms affect satellite communication systems operating between 150 MHz and 500 MHz. This band supports military applications, together with a number of civilian systems, including the Automatic Identification System (AIS) at 162 MHz, the ARGOS remote telemetry system at 402 MHz, search and rescue transponders at 406 MHz and communications to many small satellite missions. More intense storms can degrade L-band (1–2 GHz) mobile satellite communication systems (e.g. Iridium and Inmarsat) and may even affect S-band (2–4 GHz) communications. Higher frequency systems in the C (4–8 GHz), X (8–12 GHz), Ku (12–18 GHz), and higher frequency bands are unaffected by ionospheric scintillation and may be expected to keep operating normally during a severe space-weather event. Current satellite TV broadcasting in the UK uses frequencies in the Ku band.

Comparing the received signal variations, and in particular the fading, at different frequencies is difficult because of the different techniques and metrics used by different authors (Aarons, 1984; Basu et al., 1988). However, many measurements have demonstrated that when the scintillation is intense, the signal amplitude is Rayleigh distributed and this, in turn, implies that the phase is uniformly distributed over  $2\pi$ . During such periods, the ionospheric coherence bandwidth may be reduced below the signal bandwidth resulting in distortion of the signal. P. S. Cannon et al. (2006) found that the median UHF coherence bandwidth during a strong scintillation event was 2.1 MHz. It is reasonable to suppose that the coherence bandwidth will be substantially less than this during a severe event and that systems may experience frequency selective fading. The performance of systems not specifically designed to operate under such conditions is likely to be significantly impaired.

In summary, during the peak of a severe event, some satellite communication signals will experience Rayleigh amplitude fading, and coherence bandwidths will be less than 2 MHz. Due to the strength of the turbulence that generates the irregularities, these conditions will likely prevail from VHF through to S-band. P. Cannon et al. (2013) judged that scintillation may cause problems to VHF and UHF links for between 1 and 3 days, but this could be longer if multiple storms occur in succession.

### 3.3. Impacts on Global Navigation Satellite Systems (GNSS)

GNSS systems operate at frequencies between  $\sim 1.1$  GHz and  $\sim 1.6$  GHz and may employ a single frequency signal (with an associated ionospheric correction model) or signals on two or more frequencies (where no ionospheric correction model is required). Like satellite communications systems, single, multi-frequency and differential GNSS operations suffer from the effects of scintillation.

When just a single frequency is used the signal group delay and phase advance due to the total electron content (TEC) along the signal path has to be accounted for. The TEC is estimated using a model and any deviation from that model introduces errors in the receiver position, navigation and time (PNT) solutions. The model is unlikely to compensate correctly for conditions experienced during severe space weather and may underestimate or overestimate the true TEC. Mannucci et al. (2005) measured the vertical TEC observations at similar locations at the same time of day during the Halloween storms of 2003 finding that the vertical

TEC varied from a nominal 125 TECu to extremes of over 225 TECu (where 1 TECu =  $10^{16}$  electrons/m<sup>2</sup>). It follows that during severe space weather the vertical error after ionospheric model correction will sometimes be well over 100 TECu (equivalent to a range error of 16 m at the GPS L1 frequency).

Small-scale horizontal spatial gradients, which will be particularly prevalent during severe space weather, will be particularly poorly modeled. These spatial gradients will manifest as temporal gradients as the satellite being tracked moves, and this will be particularly important in some differential applications. During large ionospheric storms, the spatial ionospheric gradients at mid-latitudes can cause, at the GPS L1 frequency, excess signal delays, expressed as range errors, greater than  $400 \text{ mm km}^{-1}$  between two separated ground receivers (Datta-Barua et al., 2010). The corresponding temporal variation is a function of the satellite velocity, the frontal velocity of a moving ionospheric gradient, and the velocity of the receiver measured relative to the ionospheric pierce point (IPP). The IPP is the intersection point of a satellite-to-receiver path with a co-rotating thin shell at a nominal ionospheric altitude, for example, at 350 km. For a co-rotating receiver i.e. one that is stationary on the Earth's surface, the ray path thus moves across the co-rotating shell as the satellite moves, tracing out a track of IPP locations across the shell, at a velocity defined by the changing geometry of the ray path. Based on Bang and Lee (2013), a mid-latitude, large-storm, fixed-receiver IPP velocity of  $400 \text{ ms}^{-1}$  is reasonable resulting in a  $\sim 9.6 \text{ m min}^{-1}$  temporal gradient. Given that the Bang and Lee (2013) measurements were made during storms that were not as large as a Carrington event, we can be confident that the spatial gradient and their velocities will be higher during a severe event. Consequently, we have chosen to double both the aforementioned spatial gradient and IPP velocity for severe storms, to give a reasonable worst-case spatial gradient of  $800 \text{ mm km}^{-1}$  and a temporal gradient of  $\sim 38.4 \text{ m min}^{-1}$ .

At high latitudes, analysis of data from the October 29–30, 2003 severe storms suggests that multiple coronal mass ejections on successive days can cause daytime TEC enhancements on more than one day, and that TEC enhancements on the dayside can be convected across the polar regions into the night side polar ionosphere, causing night time disruption. These convection events can also cause significant scintillation of signals from multiple GNSS satellites (De Francesca et al., 2008).

During the storms of 2003, the GNSS Wide Area Augmentation System (WAAS), which operates over North America, lost vertical navigation capability for many hours, and the performance of differential systems was significantly impaired (NSTB/WAAS Test and Evaluation Team, 2004).

Scintillation not only reduces the accuracy of GNSS receiver pseudorange and carrier phase measurements, but it can also result in a complete loss of lock of the satellite signal. If loss of lock occurs on sufficient satellites, then the positioning service will also be lost. Conker et al. (2003) developed a very useful model to describe the effects of ionospheric scintillation on GPS availability by modeling the receiver performance and combining this with the WBMOD propagation model climatology to estimate the service availability for various levels of scintillation. The Conker et al. (2003) model illustrated that severe service degradation can occur in some regions of the world during highly disturbed periods.

During very severe storms, it is reasonable to assume that Rayleigh amplitude signal fading will prevail on most high latitude and equatorial satellite to receiver paths. However, there will probably be some less severely affected signal paths as well, enabling a few signals to be tracked and decoded. As a consequence, and noting that GNSS receiver types vary in their ability to track the satellite signals in the presence of scintillation, this suggests severely diluted precision or no positioning service at all.

The available evidence suggests that disruption to availability, accuracy, and reliability of GNSS will occur during a severe ionospheric storm event over much of the Earth. Errors will occur in single frequency receivers that rely on an ionospheric model which will be unable to keep up with the dynamics of the prevailing ionosphere, and differential (i.e. multi-receiver) systems will be unable to correct for the unusually severe spatial gradients. The impact of scintillation on a modern multi-frequency and potentially multi-constellation GNSS user is unknown, both because the spatial distribution of irregularities is unknown and because each receiver design has its own vulnerabilities and strengths. P. Cannon et al. (2013) judged that instantaneous errors in positioning of more than 100 m and periodic loss of service, lasting from seconds to tens of minutes, will occur over several days, affecting both single and multi-frequency receivers.

### 3.4. Impacts on HF Radio Communications

HF (3–30 MHz) point-to-point communications and broadcasting rely on the ionosphere to reflect radio signals beyond the horizon. The ionosphere is, however, a dynamic propagation medium that is highly challenging for HF services even during routine space weather and more so during severe events.

The principal civilian user of HF communications is the aviation industry, which employs it for aircraft flying over areas with limited ground infrastructure, e.g. over oceans. Some countries (notably the USA and Australia) also make extensive use of HF for emergency communications. The potential for space weather disruption of aviation and emergency communications by HF blackout is well illustrated by the very large solar flares of September 2017, when HF communications in the Caribbean were disrupted while emergency managers were attempting to provide support to the region following destructive hurricanes (Redmon et al., 2018).

For civilian users, HF will inevitably become less significant in future as other technologies, including satellite-based services, supplement or even displace HF. However, this will be a gradual process (c. 10–15 years) involving changes to international agreements for flight information regions, aircraft equipment, and aircrew procedures. In the interim, HF remains the primary tool for rapid voice communications between aircraft and Air Traffic Control centers for airspace management. Thus, a reasonable worst-case estimate is important as a basis against which propagation-based mitigation strategies may be judged.

#### 3.4.1. Blackout of HF Radio Communications

*Polar Cap Absorption (PCA) Events:* A PCA event results from ionization of the polar D-region ionosphere by SEPs. Ionization is caused principally by particles with energies between 1 and 100 MeV which start arriving at the Earth within tens of minutes to a few hours (depending on their energy). While the geomagnetic field shields such particles at low and mid-latitudes, they precipitate into the entire polar cap ionosphere, enhancing the D-region ionization which leads to significant levels of HF radio absorption (PCA). SEPs associated directly with impulsive X-ray flares, with no CME, produce narrow particle beams that intersect the Earth and cause PCA for only a few hours (Reames, 1999). However, SEPs produced by CME-driven shocks cover a broad range of heliospheric longitudes and their associated PCA may persist for several days (Reames, 1999; Sauer & Wilkinson, 2008). In a severe case, in July 1959, the PCA lasted for 15 days (Bailey, 1964) due to recurrent solar activity.

Riometer measurements of zenithal cosmic noise absorption at 30 MHz at 15 locations in Canada and Finland during SPEs over solar cycle 23 (1996–2008) typically ranged from 1 to 5 dB, but peaked at 19 dB during the severe July 2000 Bastille Day geomagnetic storm. Noting that dayside PCA events follow an  $f^{-1.5}$  frequency dependence (Parthasarathy et al., 1963; Sauer & Wilkinson, 2008), such an event would attenuate 10 MHz signals by more than 400 dB (peak) over a 1,000 km point-to-point communications path, rendering communications impossible. Historical observations near the peak of solar cycle 19 (1954–1964), which notably had the greatest sunspot number since 1755, showed slightly higher riometer absorption values of 23.7 dB at 30 MHz (see Table 3 of Bailey, 1964).

During severe space weather, PCAs will be more intense due to an enhanced flux of energetic particles and the region affected will extend to lower latitudes as the geomagnetic dipole field is effectively weakened by the magnetospheric ring current that develops over the course of the geomagnetic storm. Consequently, the absorption values described above can be adopted as a reasonable worst-case estimate over an enlarged polar cap.

*Auroral Absorption (AA):* AA is usually confined to geomagnetic latitudes between  $\sim 60^\circ$  and  $75^\circ$  but would be expected to move to lower latitudes and expand during a severe event. Under normal conditions, localized (200 by 100 km) absorption regions occur in the midnight sector during substorms when energetic ( $>10$  keV) electrons are accelerated from the Earth's magnetotail along magnetic field lines to the auroral zone ionosphere. This type of AA is sporadic, with events lasting tens of minutes to an hour (Hunsucker & Hargreaves, 2003). In the morning sector (6–12 MLT), and also under normal circumstances, AA is usually less localized and more slowly varying (lasting 1–2 h). It results from a “drizzle” of higher-energy (tens of keV) electrons from the outer Van Allen belt (Hartz & Brice, 1967). Auroral absorption rarely exceeds 10 dB

on a 30 MHz riometer (Davies, 1990; Hunsucker & Hargreaves, 2003) and this value is adopted as a reasonable worst-case value during a severe event.

*Sudden Ionospheric Disturbances (SIDs)*: X-rays associated with solar flares cause an increase in the electron density of the lower layers of the ionosphere over the entire sunlit side of the Earth, particularly where the Sun is at a high elevation. A single SID typically lasts 30–60 min and can shut down HF communications. During the X45 (N. R. Thomson et al., 2004) flare on November 4, 2003 (the largest in the observational record since 1974), the vertical cosmic noise absorption at the NORSTAR 30 MHz riometer at Pinawa in Manitoba peaked at 12 dB, with 1 dB absorption exceeded for ~45 min. Even the latter corresponds to > 20 dB (a factor of 100) of attenuation at 10 MHz over a 1,000 km path which, while significantly less than the corresponding PCA attenuation, is likely to close most HF communication links which have insufficient signal-to-noise margin to overcome this loss.

During a severe event, multiple flares will be expected, but the impact of SIDs will be less than PCA events, because the duration of each event is much shorter (tens of minutes, rather than hours or even days in the case of PCA events).

### 3.4.2. Anomalous HF Propagation

In addition to the D-region effects that cause signal absorption, geomagnetic storms cause many other ionospheric effects particularly in the high and low latitude F-region. In the context of severe events, these only have practical significance if the absorption does not cause a communications blackout.

At mid-latitudes, severe storms cause a significant reduction in the critical frequency of the F2-region, foF2, for periods of up to 3 days. When this happens the availability of frequencies reduces, especially during local night-time hours, and as a result of this the likelihood of interference increases. This long period of reduced foF2 may be preceded by a few hours of increased foF2 values in the early hours of the storm.

At high and low latitudes, additional reflecting structures, ionospheric gradients, and irregularities occur which affect the propagation of signals on the great circle path and deflect the signals onto non-great circle paths (Warrington et al, 1997). As a consequence, HF signals suffer unusual levels of multipath (causing frequency selective fading) and Doppler distortion of the signals. Angling et al. (1998) reported that on HF communications paths across the disturbed auroral ionosphere, Doppler spreads ranged from 2 to 55 Hz and multipath spreads ranged from 1 to 11 ms. P. S. Cannon et al. (2000) reported similar, but somewhat lower spreads on an equatorial path in Thailand. During a severe event, these spreads will likely represent a lower bound and, because the high-latitude ionosphere is likely to have expanded to mid-latitudes and the equatorial ionosphere also expanded to mid-latitudes, the anomalous propagation paths will present a major challenge to standard HF communications modems.

### 3.5. Improving Our Assessments

Estimating the expected ionospheric changes during a severe space weather event is a challenge and clearly an experimental approach is not possible. Extreme value theory is one technique that can be employed to extrapolate from minor to major events and has already had some success (e.g. Elvidge & Angling, 2018). Physics-based ionospheric modeling, whereby the physical drivers such as electric fields, winds, and composition are ramped up to values that are representative of severe storm conditions, can also elucidate the likely scenarios (P. M. Kintner et al., 2013).

## 4. Space Weather Impacts on Satellite Operations

Here we discuss how satellite operations are affected by a wide range of space weather effects including radiation, charging and atmospheric drag. This underpins a number of RWCSs as discussed in M. Hapgood et al. (2020): Section 7.3 discusses the high energy ion fluxes that produce Single Event Effects that can disrupt electronic systems; Section 7.4 discusses high-energy electron fluxes that cause internal charging leading to discharges inside or close to electronic systems with the potential to disrupt and damage those systems; Section 7.5 discusses suprathermal electron fluxes that cause surface charging leading to discharges that can generate false signals; Section 7.2 discusses the accumulation of high energy ion and electron

fluxes that is a key driver for radiation damage in electronic components and solar arrays; and Section 7.6 discusses the space-weather-driven increases in atmospheric drag that can lower satellite orbits. We also look toward an RWCS for satellite launches as the UK develops capabilities to launch satellites from its national territory.

#### **4.1. Impacts of Radiation on Satellites**

##### **4.1.1. Radiation Sources**

The high-energy radiation environment in space derives from three sources:

- galactic cosmic rays (GCRs) from outside the solar system
- radiation storms, high fluxes of SEPs accelerated near the Sun
- radiation belt particles trapped inside the Earth's magnetic field

As a result, the space radiation environment contains particles of different types and energies, and with fluxes varying on timescales from minutes to weeks and longer. This diversity leads to a wide range of effects on satellites, including single event effects (SEE), surface- and internal-charging, and also cumulative dose, as outlined below. Satellite designs mitigate these effects up to levels specified by standards such as ECSS (2008) which are based on observations of radiation environments during the space age. Therefore, severe events, larger than those observed during the space age, could exceed the normal design envelopes and push satellites into uncharted territory.

The critical parameters for this scenario are both the fluxes and fluences of particles: fluxes are a key environmental parameter to determine immediate or short-term effects such as SEE rates, while fluences (the time integrals of fluxes) are key to assessing cumulative effects such as radiation damage. In the following subsections, we discuss the environments for each effect, broadly in order of the timescales associated with their occurrence (starting with the fastest).

##### **4.1.2. Single Event Effects**

These effects are caused by  $> 30$  MeV per nucleon particles which can penetrate into the electronic devices inside spacecraft. The best evidence on the long-term occurrence of extreme fluxes of very high-energy particles comes from cosmogenic nuclides produced when they interact with Earth's atmosphere, and that are subsequently trapped in dateable natural environments such as tree rings and ice cores. Measurements of the amounts of nuclides deposited in these environments enable us to assess the occurrence of extreme events over the past several thousand years (see also Section 5). Interpolating between these measurements implies that the 1-in-100 years event could be about 2.4 times more intense than the worst events of the space age (e.g. October 1989, August 1972). Scaling the CREME96 model (A. J. Tylka et al., 1997) based on October 1989 by a factor 4 gives a 1-week worst-case fluence of  $1.6 \times 10^{10} \text{ cm}^{-2}$  at  $>30$  MeV. Scaling by a factor of 2.4 gives a fluence of  $1.0 \times 10^{10} \text{ cm}^{-2}$ , which is reasonably consistent with models that extrapolate the space age data (Gopalswamy, 2018; Xapsos et al., 2000), as well as the estimate of Cliver and Dietrich (2013) based on scaling via flare intensity. The practical advantage in using simple scaling factors on the CREME96 model is that this tool provides methods for estimating SEE rates from both proton interactions and from heavy ions and is frequently used in satellite design. Peak fluxes are important for assessing the adequacy of single event upset (i.e. bit changes in memory) mitigation techniques such as Error Detection And Correction (EDAC) codes and this is  $2.3 \times 10^5 \text{ cm}^{-2} \text{ s}^{-1}$  for 1-in-100 years, while cumulative fluences are used to assess hard failure probabilities such as burnout considered over an entire mission.

##### **4.1.3. Surface Charging**

Surface charging is due to low-energy plasma interactions with spacecraft surfaces: the relevant particles have energies up to some 10s of keV. The population is highly dynamic and the severity of charging depends on multiple environmental parameters and on many details of the interactions with surfaces. Sporadic measurements of relevant particles including electron fluxes have been available during the space age from key orbits but the complexity of the surface charging process means that defining an extreme worst-case environment is not yet possible. However, we do recognize there is an especially high risk during substorm electron injection events, when the satellite is in eclipse so there is no photoemission to counter the inflow

of electrons on to satellite surfaces. At present, a range of potentially “severe” charging environments are available in current standards, and literature, e.g. ECSS (2008), NASA (2017), Deutsch (1982), and Mullen et al. (1981), based on observations from the space age. A full analysis requires the electron spectrum over a range of energies from 100 eV to 100 keV, but Figure 8 of Fennell et al. (2001) indicates that flux enhancements in the energy range 10–100 keV are a key factor. Mateo-Velez et al. (2018) have reviewed these severe environments alongside 16 years of data at geostationary orbit data: the maximum differential flux at 10 keV found in this work is of the order  $5 \times 10^{10} \text{ cm}^{-2} \text{ s}^{-1} \text{ sr}^{-1} \text{ MeV}^{-1}$  as shown in their Figure 13, based on severe conditions reported by Gussenhoven and Mullen (1983). However, this is not an extreme value analysis, and therefore the extreme value flux for a 1-in-100 year event could well be much higher. Surface charging should be analyzed with reference to the full versions of these environments and standards.

#### 4.1.4. Internal Charging

Internal charging is caused by high-energy (>100 keV) electrons. Fluxes in specific energy ranges and in certain orbits have been observed for some decades as discussed in detail below, and more recently, some direct internal charging current observations have become available, as also discussed below. Such data have been subject to extreme values analyses in recent times that provides the basis for our reasonable worst cases for four different orbits as follows:

*Geostationary orbit:* At geostationary orbit, the daily average electron flux greater than 2 MeV for a 1-in-100 year event has been calculated as  $7.7 \times 10^5 \text{ cm}^{-2} \text{ s}^{-1} \text{ sr}^{-1}$  at GOES West and  $3.3 \times 10^5 \text{ cm}^{-2} \text{ s}^{-1} \text{ sr}^{-1}$  at GOES East (N. P. Meredith et al., 2015). These were calculated from an extreme value analysis of 19.5 years of electron data and exceed, by factors of 7 and 3, respectively, an earlier calculation (Koons, 2001), as a result of including dead-time corrections in the detector and considering the two different longitudes of the spacecraft. We also note that N. P. Meredith et al. (2015) reported the equivalent fluxes for a 1-in-150 year event:  $9.9 \times 10^5 \text{ cm}^{-2} \text{ s}^{-1} \text{ sr}^{-1}$  at GOES West and  $4.4 \times 10^5 \text{ cm}^{-2} \text{ s}^{-1} \text{ sr}^{-1}$  at GOES East. We later compare these with simulations of severe events.

None of these values are directly associated with a particular type of severe event such as a CME, being simply based on daily averages. It was shown that the maximum flux varies with longitude due to the difference between the geomagnetic and geographic equator, lower geomagnetic latitudes yielding higher flux. As a result, satellites located near 20°E and 160°W will on average experience local maxima in fluxes, with the latter being the worst-case longitude overall. For comparison, the highest observed average electron flux greater than 2 MeV was on 29 July 2004, observed by both GOES East and GOES West, and corresponded to a 1-in-50 year event.

High fluxes of these electrons typically take the form of bursts that are generated by magnetospheric processes (Horne et al., 2005) following the arrival of enhanced solar wind such as a CME or HSS. Simulations for a severe event driven by a CME show that the electron flux first drops during the main phase of the storm and is then re-formed closer to the Earth. As a result, it was concluded that the main risk of charging is to satellites in medium and low earth orbit (Shprits et al., 2011). Recent simulations for a reasonable worst case driven by a HSS lasting 5 days or more show that the electron flux can reach the 1-in-150 year event level stated above and remain high for several days (Horne et al., 2018). Thus, it was concluded that a HSS event is likely to pose a greater risk to satellites at geostationary orbit than a major CME driven event.

*Medium Earth orbit:* The maximum high-energy electron flux in the outer radiation belt varies with geomagnetic activity but usually lies between 4.5 and 5.0  $R_E$  (altitudes 22,300–25,500 km). The fluxes are conveniently ordered using the invariant coordinate,  $L^*$ , developed by Roederer for radiation belt studies (Roederer, 1970; Roederer & Lejosne, 2018). Lack of data has restricted extreme value analysis to just one or two locations along the equatorial plane. Using 14 years of electron data (2002–2016) from the INTEGRAL spacecraft, the 1-in-100 year differential electron flux at  $L^* = 4.5$ , representative of equatorial medium Earth orbit, was found to be approximately  $1.5 \times 10^7 \text{ cm}^{-2} \text{ s}^{-1} \text{ sr}^{-1} \text{ MeV}^{-1}$  at an energy of 0.69 MeV, and  $5.8 \times 10^5 \text{ cm}^{-2} \text{ s}^{-1} \text{ sr}^{-1} \text{ MeV}^{-1}$  at 2.05 MeV (N. P. Meredith et al., 2017). Note that this is differential and not integral flux. Although this analysis includes data for more than one solar cycle, geomagnetic activity was modest compared to previous cycles and may be lower than for a severe event.

An independent extreme value analysis was also performed on charging plate currents measured by the SURF instrument (Ryden, 2018) on the GIOVE-A spacecraft in a circular orbit with an inclination of 56°.

The advantage of charging currents is that they can be compared directly against the NASA and ESA design standards (ECSS, 2008; NASA, 2017). Only 8 years of data were available for this extreme value analysis, obtained between 2005 and 2016, but the results yielded a charging plate current for a 1-in-100 year event of  $0.13 \text{ pA cm}^{-2}$  (95% confidence interval from  $0.045$  to  $0.22 \text{ pA cm}^{-2}$ ) at  $L^* = 4.75$  for a charging plate located under 1.5 mm of Al equivalent shielding (N. Meredith et al., 2016a). For this level of shielding, the plate current responds to electrons above 1.1 MeV with a peak response between 1.6 and 2.1 MeV. As noted by N. Meredith et al. (2016a), a longer time series is required to improve estimates of the 1 in 100 year plate currents.

*Inner radiation belt:* Much of the published work in this area has used the McIlwain  $L$  value (McIlwain, 1961; SPENVIS, 2018), rather than Roederer's  $L^*$  coordinate noted above. This work has shown that energetic electrons capable of internal charging can be injected into the inner radiation belt ( $1.2 < L < 1.8$ ) and slot region ( $2.0 < L < 3.0$ ) by rapid compression of the magnetosphere. The fluxes of such electrons can also be artificially enhanced as a result of high altitude nuclear detonations. Observations show that electrons with energies greater than 1.5 MeV were present before such detonations in the 1960s. The resulting artificial radiation belts decayed slowly but were almost gone by 1968 (West & Buck, 1976a, 1976b). Sufficient fluxes of energetic electrons were nevertheless present in 2000 to cause internal charging (Ryden, 2018) but initial observations by the Van Allen Probes (VAP) spacecraft indicated a virtual absence of the more energetic electrons greater than 900 keV (Fennell, 2015). Temporary injections have since been observed by VAP (Claudepierre et al., 2017, 2019), but fluxes are not yet well determined. The AE8 (Vette, 1991), AE9 (Ginet et al., 2013), and CRRESELE (Brautigam & Bell, 1995) models provide the environments for the inner belt but are under review as the environment is more dynamic than previously thought. Thus, this is an area where further work is required to establish the natural 1-in-100 year event level. That work is now timely, perhaps urgent, given the growing practical interest in this region, e.g. for electric orbit raising missions (Horne & Pitchford, 2015).

*Low Earth orbit:* An extreme value analysis of satellite data at  $\sim 800$  km altitude shows that the electron flux greater than 300 keV for a 1-in-100 year event has a maximum of  $1 \times 10^7 \text{ cm}^{-2} \text{ s}^{-1} \text{ sr}^{-1}$  at  $L^* = 3.5$ . In general, there is a decreasing trend with increasing  $L^*$ , with the 1-in-100 year event at  $L^* = 8$  being  $3 \times 10^5 \text{ cm}^{-2} \text{ s}^{-1} \text{ sr}^{-1}$  (N. P. Meredith et al., 2016b).

#### 4.1.5. Cumulative Effects

Cumulative dose is due to the integrated fluences of SEPs and trapped environments as discussed above, and thus depends on the duration of the event. The dose and damage from an SEP event can accumulate over a day to a week. RWCS fluences are protons,  $>1$  MeV (for solar array damage):  $1.3 \times 10^{11} \text{ cm}^{-2}$ ; and protons,  $>30$  MeV (for aging of internal components):  $1.3 \times 10^{10} \text{ cm}^{-2}$  (Xapsos et al., 1999, 2000).

The enhanced electron flux follows several days after the geomagnetic storm and can accumulate over several days: a 1-week duration was selected for the reasonable worst case. This corresponds to  $> 2$  MeV fluences of  $4.4 \times 10^{11} \text{ cm}^{-2} \text{ sr}^{-1}$  for 1-in-100 year event, based on GOES-West. This is magnetically close to the worst-case longitude of  $160^\circ\text{W}$ , where fluences will be 1.11 greater according to the AE8 (Vette, 1991) model and 1.04 according to the AE9 (Ginet et al., 2013) model. The impact of extreme environments in GEO and MEO and the relative importance of protons and electrons for various key orbits has recently been considered by Hands et al. (2018). In interplanetary space, the entire contribution is from solar particles, while for GEO, electrons are also very significant, and for MEO orbits electrons dominate. Hands et al. (2018) have also considered the effects on solar arrays for MEO and GEO.

#### 4.2. Atmospheric Drag

As previously outlined in Section 3.1, geomagnetic storms, caused by CMEs and SIRs/CIRs, lead to joule heating and expansion of the polar thermosphere, and associated changes to thermospheric neutral density. However, during some storms, this heating is limited by enhanced radiative cooling when intense particle precipitation produces significant levels of NO in the thermosphere.

The effects of heating quickly spread to all latitudes. E. K. Sutton et al. (2009) and Oliveira et al. (2017) reported that the thermosphere response times were 3–4 h for equatorial regions and less than 2 h at other

latitudes. Largest density changes are associated with CME-driven storms, but SIR/CIR-driven storms also lead to large changes in density (Chen et al., 2014; Krauss et al., 2018). While the solar wind driving associated with a SIR/CIR is weaker than that associated with a CME, the driving lasts longer, so thermospheric density changes associated with the arrival of SIRs/CIRs are similar to those for the arrival of all but the largest CMEs. In addition, SIRs/CIRs are much more prevalent than CMEs during solar minimum, so satellite operators need to be aware of this risk at this time. Krauss et al. (2018) indicate that the larger density changes typically take place within 1 day following CME arrivals and 1–2 days for SIR/CIR arrivals. Knipp et al. (2017) showed that shock-led CMEs can lead to enhanced NO radiative cooling in the thermosphere and a curtailment of the neutral density enhancement, thus, complicating any forecast of this enhancement.

Neutral density changes associated with solar EUV variations also occur. In particular, enhancement of EUV on timescales of greater than one day, associated with strong solar active regions, can lead to neutral density increases, for a theoretical worst case, of 105% at 250 km and 165% at 400 km (Reeves et al., 2019). At the same time, transient density increases above quiet conditions, due to an assumed theoretical maximum solar flare, can be as high as 20% at 200 km, 100% at 400 km, and 200% at 600 km (Le et al., 2016). These theoretical maximum values are still considerably smaller than the extreme observed and simulated density changes associated with geomagnetic storms discussed below. Therefore, we will not consider density changes associated with EUV changes further here.

Worst-case density changes are reported in analyses of observations from polar orbiting spacecraft: that by E. K. Sutton et al. (2005), who used CHAMP observations during the October 2003 geomagnetic storm, and those by Krauss et al. (2015, 2018), who used GRACE and CHAMP observations from 2003 to 2015. The largest reported density enhancements (at 490 km) are up to 750% (relative) and up to  $4 \times 10^{-12} \text{ kg m}^{-3}$  (absolute). The impact of CIR-driven storms on density is similar to that of CME-driven storms, if the strongest 10% of the CMEs are excluded. Krauss et al. (2015, 2018) found high correlations between global neutral density and *Dst*, the hourly disturbance storm time index. It is possible to adopt the correlations calculated in Krauss et al. (2015, 2018), and extrapolate to estimate the neutral density change associated with the *Dst* estimated for our assumed worst case, the Carrington storm. However, this is likely to be questionable because of the relatively large spread in the observations used to calculate the correlations, because of the limited amount of observations available, and the sensitivity of results to the period analyzed (e.g. Krauss et al., [2018 showed different relationships between *Bz*, the north-south component of the interplanetary magnetic field, and change in density for 2003–2010 and 2011–2015 periods).

An alternative approach is to model the extreme response. Model simulations of a 1-in-100 year storm (National Science and Technology Council, 2018) indicate a fivefold increase in neutral density over the density reported during the October 2003 Halloween storm. Given that the Halloween storm was around three times stronger than quiet time conditions, this is equivalent to at least a 15-fold increase over quiet time conditions. However, these model results may suffer from using parametrizations based on observations that do not adequately represent the most severe conditions.

The Krauss et al. (2018) study benefitted from a recalibration of GRACE and CHAMP data to ensure the self-consistency of the data, and further re-calibration is required to ensure we can extend our studies to new datasets (e.g. Swarm). Further exploitation of these satellite accelerometer data, including assimilation into models, will help to improve the assessment and understanding of these very strong events on the thermosphere.

Comparison of CHAMP and GRACE data (satellites that flew at around 300–450 km and 400–500 km altitude, respectively) shows little variation in relative density changes with height. However, the reduction in absolute density with height means that drag effects are larger on CHAMP. Krauss et al. (2018) have assessed drops in satellite altitude following arrival of CMEs, with the severity of each CME characterized by the minimum value of *Bz* observed as it passed the Lagrange L1 point. They found that for severe CMEs (*Bz* = –45 to –55 nT) the altitude drops, over a 1 or 2 days following CME arrival, were 90–120 m for CHAMP, but only 40–50 m for GRACE. Such altitude changes impact satellite orbital tracking. For example, during the very large geomagnetic storm of March 13–14, 1989, tracking of thousands of space objects was lost and it took North American Defense Command many days to reacquire them in their new, lower, faster orbits. Allen et al. (1989) quote that the SMM satellite dropped ½ km at the start of the big storm and



“over three miles” (5 km) during the whole period. The drops in orbital altitude can also lead to premature re-entry for satellites already close to end of life (e.g. the Student Nitric Oxide Explorer during the 2003 Halloween Storm). Severe space weather makes prediction of both re-entry epochs and conjunctions with other satellites harder, and the latter issue may be worse in the future with the onset of new multi-satellite constellations. We need to better understand implications for satellite tracking.

#### **4.3. Space Launches**

This is an area of growing importance for the UK with confirmed plans to build a vertical launch site in the far north of Scotland and ongoing discussions to develop horizontal launch capabilities at other UK sites. It is not explicitly included as a topic in the RWCSs as shown in M. Hapgood et al. (2020), but will be considered for inclusion in future RWCSs. This will build on the issues discussed in the previous parts of this section, including:

- The radiation environments that pose a risk to space vehicles during the ascent to orbit and during early in-orbit operations that are critical to mission success, e.g. solar array deployment, ejection of shrouds, etc. Risk assessments for space tourist activities may also need this information
- The atmospheric drag environment that can disrupt assessment of the achieved orbit and hence the scheduling of early in-orbit operations. It may also affect the re-entry of discarded elements of the launch vehicle (upper stages, shrouds, etc.)

### **5. Space Weather and Atmospheric Radiation**

Here we discuss the enhanced levels of atmospheric radiation that can arise from an SEP event with significant fluxes of particles with energies  $> 400$  MeV, and that can affect operations of aircraft and of electronic devices on the ground. This underpins a number of RWCSs as discussed in M. Hapgood et al. (2020): Section 7.15 discusses the neutron fluxes that can lead to significant rates of single event effects in avionics, Section 7.16 which discusses how these neutron fluxes can accumulate to deliver significant radiation doses to aircrew and passengers; and Section 7.7 which complements Section 7.15 by discussing the ground level neutron fluxes that can lead to SEEs in electronic systems on the surface of the Earth.

#### **5.1. Introduction**

When high-energy particles strike the Earth's atmosphere they can interact with the nuclei of oxygen and nitrogen to generate a cascade of secondary particles including neutrons, protons, electrons, and muons. The secondary radiation builds up to a maximum at around 60,000 feet (18 km) and then attenuates down to sea level. This secondary radiation includes both a slowly changing background due to GCRs and episodic increases when SEP events contain significant fluxes of very high-energy particles. Secondary radiation from particles with energies above 400 MeV can reach aircraft cruising altitudes and sea level. The latter class of events occurs approximately once per year and is known as a ground level enhancement (GLE).

The secondary radiation from GCRs is an important practical issue for aviation. However, it is a continuous effect, slowly changing in response to changes in GCR fluxes; thus, we do not consider it as part of this worst-case scenario. Rather, we focus on the enhanced secondary radiation fluxes generated by SEP events.

#### **5.2. Effects on Civil Aviation**

The awareness of the possible impacts on people at aviation altitudes dates to the 1960s (Armstrong et al., 1969; Foelsche, 1962, 1964), with the emphasis at that time being on the development of supersonic passenger travel, because such aircraft would need to fly higher. However, in the 1960s, radiation protection for both workers and the public was in its relative infancy, with modern style dose limits for people not being introduced until 1977 (ICRP, 1977) with updates following in 1990 (ICRP, 1991) and 2007 (ICRP, 2007). More recently, the International Commission on Radiological Protection (ICRP) have made specific recommendations for air crew (ICRP, 2016).

Since the late 1980s there has also been increasing awareness of the threat posed to electronics by single event effects (SEEs), caused by the atmospheric radiation environment produced by galactic cosmic radiation, e.g. (C. S. Dyer et al., 1989; Normand, 1996; Ziegler, 1996). Such effects are identical to those occurring in space systems and are more fully discussed in P. Cannon et al. (2013), and in the various standards, e.g. JEDEC (2006) for sea-level soft errors (i.e. SEE-induced changes to data and/or code within electronic devices), and IEC (2016) for effects at aircraft altitudes.

Early attempts to consider the influence of GLEs, such as C. S. Dyer et al. (2003), have recently been greatly improved (C. Dyer et al., 2017), by updated modeling of the largest event directly measured on February 23, 1956 and by generation of the size distribution, using recent events directly observed since 1942, together with evidence for historic events from cosmogenic nuclides, which were first noted by Miyake et al. (2012). The early ground monitoring by ionization chambers has been reviewed by Shea and Smart (2000), and the first ground level enhancements of 1942 and 1946 were announced by Forbush (1946). Subsequent observations since 1948 were made using ground-level neutron monitors invented by Simpson, as described in his later review (Simpson, 2000). By 1956, there were some 17 monitors active when the largest event of modern times occurred on February 23, 1956 (Rishbeth et al., 2009) (this event will subsequently be abbreviated as “Feb56”), when the maximum measured increase was at Leeds UK, where neutron fluxes some 50-times greater than background levels were reached within 15 min (this was the time resolution of the monitor at the time).

Before 1942, we have only indirect measurements of cosmic radiation and solar particle events from cosmogenic nuclides such as  $^{10}\text{Be}$  and  $^{36}\text{Cl}$  in ice cores, and  $^{14}\text{C}$  in tree rings. These results (Mekhaldi et al., 2015) indicate an event some 30 times greater than the Feb56 GLE in 774 CE, and another, 15 times greater than Feb56, in 994 CE. The nuclides from these events were detected at enhanced levels in geographically widely dispersed ice core drillings and tree ring samples, and the relative amounts of  $^{36}\text{Cl}$  and  $^{10}\text{Be}$  imply that these large events had hard spectra, similar to GLEs in February 1956 and January 2005. While the 1859 event does not show as a significant feature, there appear to have been some seven events per century in the range 0.5–1 times the Feb56 GLE, between 1800 and 1983 (K. G. McCracken and Beer, 2015). The absence of any cosmogenic nuclide signal from 1859 is probably due to the location of the flare event at  $10^\circ\text{W}$  on the Sun. This is a favorable location for major geomagnetic storms from CMEs, but not for major particle events that originate further westward (e.g.  $80^\circ\text{W}$  for February 1956).

C. Dyer et al. (2017) provide probability distributions for event sizes using data from Duggal (1979) and K. G. McCracken et al. (2012) combined with cosmogenic nuclide data from Miyake et al. (2012) and Mekhaldi et al. (2015). The cosmogenic nuclide data and the implications for space weather effects have recently been extensively reviewed in the book by Miyake et al. (2020). There is tentative evidence of a turnover for very large events, which is consistent with Usoskin and Kovaltsov (2012), who find no evidence for events beyond 50–100 times Feb56. Interestingly, interpolating between the direct measurements and cosmogenic data suggests that the occurrence rate of a 2.4 times Feb56 event is around 1 per 100 years, so that although the Carrington event itself was not very intense at high energies, the use of 2.4 times Feb56, for 1 in 100 years events, appears reasonable.

In C. Dyer et al. (2017), the Feb56 GLE was characterized in detail, to serve as a yardstick for quantifying hazards, based on the A. J. Tylka and Dietrich (2009) global average spectrum.

In the RWCS tables in M. Hapgood et al. (2020), we present secondary particle fluences and dose equivalent rates in polar regions for events recurring every 100 years, and also every 150 years. The energy threshold of 10 MeV for neutrons is commonly used in the literature and in standards as single event effects commonly have cross-sections that plateau above this energy, and fall-off rapidly below. Protons also give nuclear interactions producing SEEs but with a higher threshold energy (some 20 MeV). Local conditions (hydrogenous materials) can thermalize the low energy neutrons and this can greatly enhance SEE rates in certain electronic components that contain the  $^{10}\text{B}$  isotope of boron (20% of naturally occurring boron). For many modern devices, with very small feature sizes, direct ionization by protons and muons can deposit sufficient charge to lead to SEEs.

The work of C. Dyer et al. (2017) also presents a worst-case time profile based on the recent work of McCracken et al. (2016) using ionization chamber data, which had analogue outputs and hence improved time

resolution compared with the neutron monitors of the time. Peak rates are enhanced by about a factor of 3, compared with the hourly average rates.

The influence of radiation dose on crew and passengers should also be considered with regards to operational airline planning and public health protection, reflecting the public health principle of keeping radiation exposure as low as reasonably achievable (CDC, 2015; ICRP, 2007). For instance, an event comparable to Feb56 could give  $\sim 7$  milliSieverts (C. Dyer et al., 2017), or 35% of the annual dose limit of 20 milliSieverts (ICRP, 2007) used in Europe for aircrew (Euratom, 1996, 2013) in a single high-latitude 40,000 ft (12 km) altitude flight: this is above the dose levels at which airlines sometimes re-roster crew to lower dose activities in order to keep annual dose below 6 milliSieverts, the level at which crew are required to be classified (Air Navigation Order, 2019). Classified workers are subject to annual medical examinations and additional training requirements, and dose record-keeping, all of which have added cost implications. Dose limits do not apply to passengers, but there will be public concern about the receipt of such a dose.

For a 1-in-150 years event, the doses received could reach  $\sim 28$  milliSieverts (C. Dyer et al., 2017), about 1.4X the occupational dose limit. Both a Feb56 and a 1-in-150 year event may cause operational difficulties for airlines, since crew may have come close to, or exceeded, their annual dose allowance. For a 1-in-1,000 year event, the distribution given in C. Dyer et al. (2017) implies radiation levels some 20 times Feb56, so that the doses could reach 150 milliSieverts. Even at this level, no acute, short-term effects would occur, but those exposed would have a small increased lifetime risk of stochastic effects, such as cancer: the threshold for acute effects is more than an order of magnitude higher, but an individual receiving 150 milliSieverts will have an increase of about 1% in their lifetime risk of fatal cancer.

It is hard to estimate exactly how many people could be exposed to these levels of radiation because it will depend on the global range and duration of the high-dose rates, and whether airlines have modified their flight patterns in response to the perceived risk. However, the number of people exposed could exceed 10,000, with one estimate putting the number at 13,000 (P. Cannon et al., 2013). Experience from nuclear accidents shows that the public can be very concerned about exposures to ionizing radiation, and at times of heightened solar activity, media coverage has concentrated on the prospect of radiation doses; significant public concern can be anticipated. However, at such dose levels, there would be more severe operational problems for airlines. In addition, the SEE rates in aircraft engine and flight systems could pose a very significant challenge to flight safety, especially as decreasing feature sizes in avionics systems may increase vulnerability to SEEs (P. Cannon et al., 2013; IEC, 2017).

Many flights now reach 43,000 ft (13 km) altitude for which flux rates increase by about 30% with respect to 40,000 ft (12 km) and executive jets reach 49,000 ft (15 km), so dose rates would be higher in both those cases. Dose gradients with respect to altitude are very steep, for example for Feb56 a factor 15 between 40,000 ft and 20,000 ft (6 km), and a factor of 3 between 40,000 ft and 30,000 ft (9 km), at 80° North. As a result, flying at lower altitudes is highly beneficial, if alerts can be provided in time, and Air Traffic Control is able to coordinate emergency descents to ensure safe separation is maintained between aircraft, and that aircraft have sufficient fuel.

The dependence of neutron fluxes on altitude for several GLEs and for cosmic rays is given in detail in C. S. Dyer et al. (2003). It should be noted that the altitude gradients vary with geomagnetic latitude and differ somewhat between different particle species and even between the different dosimetric quantities. For accurate assessment of the advantages of altitude and route variation, use should be made of the detailed models available (e.g. Models for Atmospheric Ionizing Radiation Effects, MAIRE, see <https://www.rad-mod.co.uk/maire>).

The International Civil Aviation Organization (ICAO) has recently published the first suggested solar radiation storm hazard levels, but recognizes that more scientific rigor and detail needs to be brought forward to improve operational and health decisions (ICAO, 2018, 2019): their recommended threshold for severe events is  $80 \text{ microSieverts h}^{-1}$ , which could be breached during many radiation storms with hard SEP spectra (and that also produce GLEs). If this recommended threshold is applied, the impact may be financial rather than connected to increased risks to passengers and crew.

There is also a strong latitude gradient (for example, a factor of 18 between 80° North and 51° North, along the Greenwich meridian at 40,000 ft) and this can be exploited to reduce the radiation hazard. However, it should be noted that if a severe geomagnetic storm is in progress this advantage is greatly diminished because the storm reduces the ability of Earth's magnetosphere to deflect energetic particles, and thus enables them to reach lower latitudes than would be possible under quiet geomagnetic conditions. An example of this reduction in geomagnetic shielding of energetic particles was observed in flight data during the GLE of October 24, 1989 (Dyer et al., 2003, 2007). The simultaneity of geomagnetic storms and atmospheric radiation increases due to SEP events is probably quite common and should be explored further. It was certainly evident for the GLEs of November 1960 and December 2006. Indeed, for the Carrington event virtually no geomagnetic protection can be assumed, as aurorae were seen in the tropics (Green & Boardsen, 2006).

### 5.3. Effects on Terrestrial Electronics

Sea-level ambient dose equivalent rates from a Feb56 event are low (2.5 microSieverts per hour) even at the poles where there is no geomagnetic shielding, and even lower (0.6 microSieverts per hour) at the latitude of the UK; these levels are of little concern. However, SEE rates could be of concern for safety-critical systems such as nuclear power, national grid, railways and autonomous vehicles (whether cars, ships or aircraft), particularly for 1-in-150 or 1-in-1,000 year events. The implications for ground level infrastructure have been extensively discussed in A. Dyer et al. (2020).

## 6. Solar Radio Burst Impacts on Radio Systems

Here we discuss how strong signals from solar radio bursts can inject spurious signals into radio and radar receivers, and potentially interfere with the intended signals that those receivers are seeking to collect. This underpins RWCS Section 7.8 which assesses the strength of those radio bursts and whether they can interfere with a number of different radio technologies (e.g. GNSS, aviation control radars, etc.).

The Sun has long been known to be an important source of radio noise (Hey, 1946), and can sometimes produce intense bursts of radio noise that disrupt wireless systems. These solar radio bursts (SRBs) are often associated with the launch of CMEs or the energization of electrons by plasma processes (e.g. magnetic reconnection or shocks) in the solar atmosphere (Bastian, 2010).

SRBs have the potential to affect a wide range of terrestrial and space-based radio systems. Like D-region absorption in HF systems, SRBs reduce the signal-to-noise ratio (SNR), but do so by increasing the background noise. The level of impact is determined by the intensity and duration of the SRB, the technical characteristics of the affected radio system, and whether the receiving system is pointing toward the Sun. Bala et al. (2002) examined over 40 years of SRB data to determine the duration of the events and their intensity, finding that 50% had a duration > ~12 min and 30% had a duration > ~25 min at frequencies above 1 GHz.

Using the equations given in Bala et al. (2002), SRBs with an intensity of ~1,000 SFU (1 SFU =  $10^{-22}$  W m<sup>-2</sup> Hz<sup>-1</sup>) should cause more than a 3 dB (noticeable) increase in noise at cellular mobile base stations at dawn and dusk, when the antenna is pointing toward the Sun (at 900 MHz, assuming an antenna gain of 16 dB and a receiver noise figure of 2 dB). Bala et al. (2002) also determined that in the period 1960–1999 there were 2,882 SRB events (assuming a 12-min window) with an intensity >1,000 SFU, i.e. more than one per week. However, somewhat surprisingly, there is only one published report of an SRB impact on a cellular mobile system (Lanzerotti et al., 1999).

Moreover, no issues have been reported in the literature for the largest SRB on record, which occurred between 19:30 and 19:40 UT on December 6, 2006, and which exhibited an intensity of more than one million SFU. Again, adapting the equations provided by Bala et al. (2002), the base station noise level should have increased by ~35 dB from the pre-SRB level (at 900 MHz, assuming antenna gain 16 dB, receiver noise figure of 2 dB), and the mobile noise level should have increased by ~14 dB (at 900 MHz, assuming an antenna gain 0 dB, noise figure of 6 dB). In the context of a base station, with its horizontally directed antennae, the absence of any recorded issues is understandable because the Sun was not close to the horizon over any major populated region. Mobiles though, unlike base stations, have no such constraint on solar elevation, and the lack of any reported issues may be due to commercial sensitivity.

In contrast, the December 2006 SRB event did cause outages in the International GNSS Service (IGS) network, WAAS, and other GNSS networks (Cerruti, 2008). Those networks use semi-codeless receivers that have enabled civil access to dual-frequency GNSS measurements without full knowledge of the pseudorandom codes embedded in GNSS signals; however those receivers are more vulnerable to reductions in the SNR than code-tracking receivers (which have knowledge of those codes). Carrano et al. (2009) also reported substantial degradation of tracking and positioning by AFRL-SCINDA receivers during the December 6 SRB event, but less significant degradation during the other less intense SRB events that same month. Mobile satcom (UHF and L-band) operation may also be affected by SRBs. Similar to cellular communications the impact of SRBs is likely to be highly dependent on the design of individual systems. No recorded impacts have been identified, but technical analysis suggests impacts are possible for geostationary satellites around equinox, when the satellites lie close to the direction of the Sun (at certain times of day), and for mobile systems with large beamwidths and low link margins (Franke, 1996).

There is also practical evidence that radars monitoring air traffic can be disrupted by SRBs. This was the basis of the early SRB impacts noted above (Hey, 1946), where SRBs interfered with military radars. These impacts have generally been well-mitigated in recent decades, but an incident in November 2015 showed that we need to maintain awareness of this potential impact. During that incident, an intense SRB (around 100,000 SFU at 1 GHz) caused extensive interference to air traffic control radars in Europe, generating many false echoes in radars in Belgium, Estonia and Sweden, and has been discussed by Marqué et al. (2018). In Sweden, these echoes caused the air traffic control system over the south of that country to shut down for several hours, severely disrupting flights not just in Sweden, but also those transiting Swedish airspace. It also prompted a major security alert, given the role of aviation as a critical infrastructure.

In conclusion, the event on December 6, 2006 sets a lower boundary for a severe SRB event and consequently, our reasonable worst-case SRB intensity is set at 2 million SFU with a period of 20 min above this threshold. The consequence is likely to be short-period degradation of GNSS systems and some mobile cellular networks. There is also potential to disrupt air traffic management if aviation radars are not operated with an awareness of SRBs. There is further potential for impact on satellite communications, but this has not been demonstrated in the course of operations.

## 7. Cross-Cutting Issues

As we indicated in Section 1.2, many of the impacts discussed above will occur close together in time because of the interconnections between the space weather effects that cause these impacts. Thus, it is essential to provide the users of individual RWCSs with insights into these interconnections, so they can appreciate how adverse impacts on their activities are linked with impacts on what appear to be very different activities.

For example, during a geomagnetic storm, we may expect to see impacts that include: (a) GICs in a range of engineered systems, (b) changes in satellite drag, (c) disruption of key radio technologies including GNSS, HF communications, and VHF/UHF/L-band satellite links, and (d) increased anomalies on satellites, particularly those exposed to the outer radiation belt (i.e. geosynchronous and medium Earth orbits). So it is important to outline to RWCS users how these diverse impacts will all arise during the course of a severe geomagnetic storm, as magnetospheric processes interact with the ionosphere and thermosphere. Thus, all the RWCSs that arise from geomagnetic storms can occur at more or less the same time. There may be some phasing with some effects arising early in the storm and others later. But the bottom line is that these RWCSs should be considered as an ensemble when assessing the potential impact of a severe space weather event. They will occur close together in time with the order determined by the sequence of events on the Sun.

A solar radiation storm will also produce a range of effects, but these will depend on the energy of the solar energetic particles that form the storm and the location at which the effect is experienced. We may expect to see impacts that include: (a) increased anomaly rates and radiation damage on satellites, particularly on those in high orbits such as geosynchronous, which are fully exposed to high energy particles coming from the Sun; and (b) a blackout of HF communications in polar regions. If the storm has significant particle fluxes above 400 MeV, there will also be an atmospheric radiation storm (i.e. enhanced fluxes of energetic

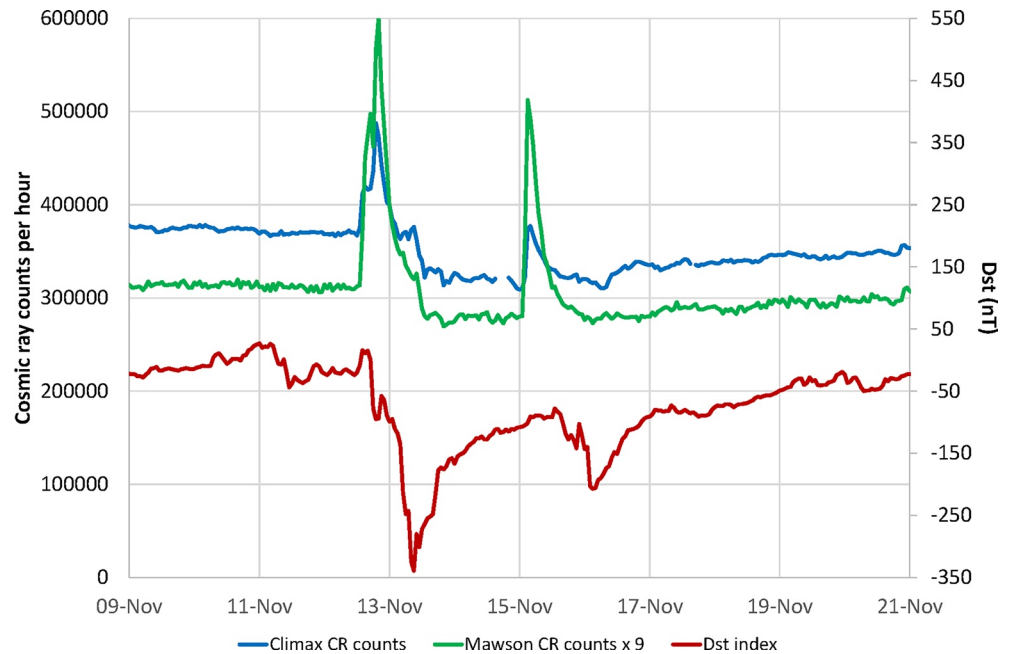


**Figure 3.** A concrete example that the onset of geomagnetic and radiation storms can coincide due to the timing of two separate bursts of solar activity. A very large geomagnetic storm started on November 12, 1960 with a sudden commencement at 13:48 UT, indicating the arrival of a large coronal mass ejection (CME) at Earth, as shown by a brief rise in the ring current index, *Dst*, followed by a large decrease in *Dst* during the main phase of the storm. At almost exactly the same time, an intense radiation storm started, leading to a ground level enhancement (GLE) of radiation as seen here in data from ground-based cosmic ray (CR) monitors at Climax in Colorado, and Mawson in Antarctica. (Note that the Mawson CR counts have been increased by a factor of 9 to facilitate plotting on the same scale as Climax data; Climax is a high altitude (3,400 m) site so experiences much higher cosmic ray counts than the sea-level site at Mawson.) The radiation storm was associated with intense solar flare and radio burst activity that was first observed around 13:20 UT the same day (NOAA, 1960). The CME launch was probably associated with solar flare activity around 03:00 UT on the previous day, as indicated by a major blackout of high frequency (HF) communications in East Asia and Australia (NOAA, 1961); no direct solar flare observations were available at that time (NOAA, 1960). The figure also shows that there was further solar activity leading to another radiation storm on 15 November and another geomagnetic storm (dip in *Dst*) on 16 November.

neutrons), leading to (c) increased anomaly rates and some potential for damage to avionics, (d) increased radiation doses accumulated by aircrew and passengers, perhaps giving a small increase in lifetime risk of cancer, and (e) enhanced rates of single event effects in electronic systems on the ground (but no significant impact on human health). So it is equally important to outline to RWCS users how this other set of diverse impacts will all arise close together in time, but in this case as the result of a severe radiation storm. Thus, we have a second set of RWCSs that should be considered as an ensemble when assessing the potential impact of a severe space weather event.

While there are some overlaps between the two ensembles in that they can both disrupt satellite operations and radio systems, it is important to recognize that there are also major differences between the two ensembles, especially in terms of their solar-heliospheric drivers: CMEs and SIRs/HSSs, on the one side, and, SEPs on the other side. These different physical drivers mean that the two ensembles do not necessarily occur simultaneously and one must be cautious in making links between the two. For example, experience shows that some users may mistakenly associate GIC and atmospheric drag with radiation storms. Thus, we need to provide clear advice that can avoid such misunderstandings.

Nonetheless, strong solar activity leading to severe space weather is highly likely to cause both geomagnetic and radiation storms over the course of multiple days. It is also possible (there are examples in the 20th century observational record such as that shown in Figure 3) that major solar events a day or so apart can cause the simultaneous occurrence of a severe radiation storm and a severe geomagnetic storm at Earth. In these cases, the radiation fluxes reaching the atmosphere will be enhanced since, during geomagnetic

storms, the magnetosphere is more open to inflows of energy and particles coming from the Sun, e.g. as in a radiation storm on October 24, 1989 studied by C. S. Dyer et al. (2003). Thus, the potential for geomagnetic and radiation storms to occur close in time reinforces the importance of considering space weather RWCSs as an ensemble.

## 8. Public Behavior

Here we assess how public behavior may respond during a severe space weather event. RWCS Section 7.17 summarizes the points raised here.

In 2017, with much encouragement from Government, we started to extend the space weather RWCSs to include an assessment of public behavior in response to severe space weather. This human environment cannot be characterized in the same way as the physical environments discussed in previous sections, but is closely linked, both as a human response to the consequences of those environments, and as a response that can be influenced by an appreciation of scientific understanding of those environments. Therefore, we have developed a narrative assessment as follows.

Public behavior, particularly after a severe space weather event, is difficult to predict as the frequency of such events does not give us a robust baseline. The 1859 Carrington Event preceded most of our contemporary technologies and it is hence hard to draw public behavior lessons from this (Cliver & Svalgaard, 2004). In practice, much will depend on the scale of the event. For example, the 1989 geomagnetic storm that caused a blackout in Quebec, closing schools and businesses, did not result in notable public behavior anomalies, but in this case the impact on the electricity grid was short lived (Béland & Small, 2004).

Severe space weather is a High Impact, Low Probability event where there is little public understanding of causes and consequences. A telephone survey of 1,010 adults in England and Wales conducted in 2014 found that 46% of the sample had never heard of space weather and an additional 29% had heard of it but know almost nothing about it (Sciencewise, 2015). It has been suggested that expectations of greater civilian activity in space might increase public knowledge and interest in space weather (J. Eastwood, 2008) and so we may see knowledge increase over time. Scientific understanding of space phenomena can be undermined by conspiracy theories which may propagate online through the echo chamber effects of social media. For example, online rumors concerning the existence of a so-called “Planet X” or “Nibiru,” which will collide with Earth have circulated online since 1995 despite the absence of scientific evidence (Kerr, 2011).

How the public would react to the secondary consequences of space weather, primarily its impact on infrastructures (such as the electricity grid or telecommunications – P. Cannon et al., 2013) is reasonably well understood. A recent comparison (Preston et al., 2015) of international case studies of public behavior in infrastructure failure shows that communities will usually react responsively and pro-socially with at least neutral, or even positive, impacts on social cohesion. Communities would only be expected to react negatively to official help and advice in a space weather event (reframing) when they consider that the official response is not equitable. For example, if power is restored to communities in a way that is perceived to be unfair then it is likely that there will be negative political consequences that may result in demonstrations or public disorder (Preston et al., 2015).

Space weather would result in an increased demand for essential goods and services with associated stockpiling by consumers. Goods that are stockpiled usually include petrol, bottled water, canned goods and toilet paper. Stockpiling is a rational behavior in disasters and emergencies and is not a problem as long as retail stocks and supply chains are not compromised. However, if people consider that stocks and supply chains may be compromised in the future, or that they need excess supplies at home for an anticipated event, this may increase demand to the extent that it outstrips supply. This can become a self-fulfilling prophecy as in the COVID-19 pandemic when in March 2020 many supermarkets were experiencing shortages. Fear of shortages leads to stockpiling which in turn leads to shortages that exacerbate demand through (so-called) “panic buying” (which is a misnomer for the rational purchasing behavior that actually occurs, see Drury et al., 2013) resulting in further shortages. Prices may rise rapidly, queuing may occur, stocks can be depleted and (rarely) some individuals may resort to theft to obtain supplies. Supply chains in the UK are lean (i.e. little stock is held) and are particularly vulnerable to excessive buying in a crisis (House of Lords

Scientific Committee, 2005, p. 124). We may therefore expect consumer behavior to be self-reinforcing if there are media reports of queues or shortages following (or just before) a space weather event.

We know very little about how the specific context of a space weather event (the fact that it emerges from space) might impact on public behavior. There may be something unusual about the context of space weather, as 35% of respondents in the Sciencewise (2015) study would be more concerned about a power cut in their area caused by space weather when compared to other causes. Unlike an accidental event, or malicious attack, some fringe groups might consider that there is a particularly apocalyptic message behind a space weather event. At the extremes, this may lead to unusual forms of behavior. Millenarianism refers to a view of certain religious sects, or individuals, who consider that certain events are a sign that the world is coming to an end. These events are often linked to space events such as comets (McBeath, 1999) and pseudo-scientific concepts such as changes in “galactic alignment” or cataclysmic “pole shifts.” Sometimes religious cults use space events as a justification for mass suicides or violent events. For example, the 1999 suicide of 31 members of the “Heaven’s Gate” cult in San Diego, California was planned after their observations of the Hale-Bopp comet in 1997 (the cult believed a spacecraft trailing the comet would take them from Earth). Fifty-three members of The Order of the Solar Temple, who worship the Sun, died in Switzerland in 1994 (Palmer, 2016). There is a distinction between these cults as “Heaven’s Gate” were motivated by a specific space event whereas The Order of the Solar Temple were more generally motivated by recurrent events such as the solstice. Many of these deaths were not necessarily suicide and resulted from the murder of their own members. Such events are extreme and difficult to predict but may coincide with a solar event such as severe space weather. We would highlight the specific “space” focus of many contemporary cults, and conspiracy theorists, as an area of concern during a space weather event.

### 8.1. Anxiety

The UK National Risk Assessment (Cabinet Office, 2017) recognizes that one key element in the impacts of natural hazards is the psychological impact on the wider population, including widespread anxiety. Anxiety is an important psychological impact as it can impose large costs on society and the economy, in particular through lost employment, but also through the costs of treating anxiety (McCrone et al., 2008). Anxiety is likely to arise during severe space weather through several mechanisms, in particular loss of electric power. This is supported by the Sciencewise (2015) public dialogue study discussed above; during this study the public response always focused back on loss of electric power as the primary concern. There was a clear recognition by members of the general public that their lives would be severely disrupted by loss of this technology, much more so than loss of GNSS or even aviation radiation risks. The Sciencewise study also highlighted that the public recognized the value of good honest advice in dealing with the impacts of space weather. The risk of anxiety during a severe space weather event can be reduced by providing good transparent information, and where feasible, engaging in dialogue. Conversely, it can be magnified by poor information, whether overly optimistic or overly pessimistic, and, perhaps even worse, by a lack of information.

## 9. Discussion

Severe space weather was formally recognized as a significant natural hazard in the UK in 2011, because scientific evidence, as outlined here, showed that severe space weather conditions are to be expected on similar timescales to extremes of other natural hazards considered in the UK National Risk Register (Cabinet Office, 2017). This was strongly complemented by engineering assessments that demonstrated that the operation of many critical national infrastructures might be disrupted in these severe space weather conditions (P. Cannon et al., 2013). The recognition of space weather as a significant risk was reinforced by the uncertainties noted in both sets of evidence, i.e. these uncertainties were recognized as a further risk factor.

Since that time, there has been significant progress in resolving some of those uncertainties, as shown by many of the post-2011 references cited in this paper. A prime example is progress in understanding the size and likelihood of very intense atmospheric radiation storms following the detection of cosmogenic isotope signatures of several such storms over the past 3,000 years (Mekhaldi et al., 2015; Miyake et al., 2012; O’Hare et al, 2019). These new data have helped to put the limited observational record (~80 years) in a longer-term context, giving better insights into the centennial timescale risk from atmospheric radiation storms (Dyer



et al., 2017, 2020). Another important example is in better understanding the nature of the risk posed by GICs: (a) the importance of ground and sea conductivity in creating the geoelectric fields that drive these currents (Kelly et al., 2017; Pulkkinen et al., 2017); (b) that the large geomagnetic variations ( $dB_H/dt$ ) that create the most intense geoelectric fields can often occur as short bursts, sometimes with limited (a few hundred km) spatial extent (Cid et al., 2015; Ngwira et al., 2015; Pulkkinen et al., 2015); and (c) that large geomagnetic storms will generate multiple instances of such bursts, generally at different locations, and at different times within the storm (e.g. Boteler, 2019; J. P. Eastwood et al., 2018; M. Hapgood, 2019a; Oughton et al., 2019). This better understanding has the potential to enable improved modeling and forecasting of the impacts of large GICs on all electrically grounded infrastructures.

These are just two examples of improved understanding of space weather environments. Other examples include better assessment of charged particle environments in space, through the provision of better quality data and through the use of extreme value statistics. But there remains much scope for further improvement in all these areas, e.g. to exploit newly exposed data on historical events such as the 1770 geomagnetic storm (Hayakawa et al., 2017) and the ~660 BC radiation storm (O'Hare et al., 2019), as well as deeper analyses of existing datasets. Another important area for future work is to understand better the physics at work in extreme space weather conditions, e.g. a highly compressed magnetosphere as during the August 1972 storm (Knipp et al., 2018) and to incorporate that knowledge in models of severe space weather. This approach mirrors work to simulate extreme tropospheric weather such as hurricanes (Smith, 2006) and has the potential to simulate future events that human societies may otherwise have to wait decades or even centuries to experience (M. A. Hapgood, 2011).

The need for improved understanding of space weather is recognized by UK funding bodies, as demonstrated by recent support for a wide range of research projects in key areas such as GICs, radiation effects on satellites and on ground-based infrastructures. A very recent major step forward was the September 2019 announcement of £20 million funding for the Space Weather Instrumentation, Measurement, Modeling and Risk (SWIMMR) project (<https://www.ralspace.stfc.ac.uk/Pages/SWIMMR.aspx>). This will support a range of projects, with an emphasis on work that transitions space weather models into operations and develops new UK space-weather monitoring capabilities that will feed data into those operations. It is important to recognize that the need for improved understanding is not limited to the refinement of existing evidence. Our society's vulnerability to space weather is ultimately driven by our growing dependence on advanced technologies to deliver services used in everyday life (M. Hapgood, 2019b). Thus, we need to monitor emerging technologies to understand whether they are vulnerable to space weather and, if so, to determine what extreme environments they will encounter. A prime example today is the development of autonomous vehicles (cars, ships, and aircraft) where GNSS is an important (but not sole) element in vehicle navigation, and, hence, there is a potential space weather vulnerability arising from ionospheric impacts on GNSS. This need to monitor emerging technologies is complemented by a need to maintain awareness of space weather as existing technologies are refined, lest new vulnerabilities are inadvertently created. A modern example of this issue is the November 2015 disruption of air traffic in Northern Europe, when a large solar radio burst generated large number of false signals in radar systems in Belgium, Estonia, and Sweden (Marqué et al., 2018). The potential for radar interference from the Sun has been known for over 70 years (Hey, 1946) but was clearly missed in this case, so the lesson was re-learned the hard way. As a result, we have included the risk of radar interference in our set of reasonable worst-case scenarios. It is a risk that is generally well-mitigated, but does need to be included in our scenarios so as to support that mitigation.

Moving away from individual risk factors, we must recognize that these impacts on different technologies will occur close together in time, most obviously as a magnetically complex active region crosses the face of the Sun as seen from Earth (as happened in major past events such as that of March 1989). Thus, the range of adverse space weather environments, as discussed in Sections 2–6, need to be considered both individually (for their impacts on specific technologies) and as an ensemble that will all occur during a future major event, as we note in Section 7. It is this ensemble that will disrupt a diverse host of societally vital infrastructures including energy, communications, and transport. Thus, it is important to provide policy-makers with cross-cutting scenarios, such as that in P. Cannon et al. (2013), that highlights such ensembles.

Another cross-cutting issue that we have considered is public behavior, i.e. to consider how people may respond when a severe space weather event next occurs. This is recognized by the UK Government as an

important element of the wider environment within which major risks affect society. We have, therefore, included this in our assessment, taking account of studies that have explored how the public can engage with space weather (Sciencewise, 2015), and also of wider studies on the public behavior in response to unusual but stressful events. These make it clear that the public value good, honest and transparent advice from experts and Government, and that this can reduce the anxiety that naturally arises when people face serious risks. However, further work is needed to explore how best to provide that advice, recognizing that for severe space weather, communications may be disrupted. We anticipate that this will become an important area for future work, given that the 2020 COVID-19 pandemic is likely to stimulate a wider focus on the communication of information about societal risks and their impacts on everyday life. It will be important to understand where space weather can have similar societal impacts to those seen during this pandemic, e.g. the disruption of supply chains for some products, and also to understand where space weather can have opposite societal impacts. For example, the COVID-19 pandemic has led to greater use of cashless transactions, but severe space weather is likely to disrupt electronic payments systems (Haug, 2010), thus, driving a switch back to cash.

In summary, this paper outlines how we have developed a set of reasonable worst-case space weather scenarios that can assist UK policy-makers in planning for the impact of severe space weather on our country. We provide both specific scenarios for a wide range of critical technologies, and cross-cutting views of how these scenarios could combine to create greater risk during a severe space weather event. We also consider public behavior in response to information about an event and note that good messaging is critical to helping people to deal with the stress that will naturally arise.

Finally, while the target for these scenarios is the UK, we note that they contain many ideas that may be of assistance to other countries. We welcome and encourage productive dialogue with other countries, and recognize the valuable role of international discussions that have already occurred, e.g. support for the development of the US Space Weather Benchmarks (National Science and Technology Council, 2018; Reeves et al., 2019).

## Data Availability Statement

Figure 3 is generated for this paper using *Dst* index from the World Data Center for Geomagnetism in Kyoto (see <http://wdc.kugi.kyoto-u.ac.jp/dstdir/>), and cosmic ray data from the World Data Center for Cosmic Rays in Nagoya (<http://cidas.isee.nagoya-u.ac.jp/WDCCR/>). Sudden commencement times were sourced from the International Service on Rapid Magnetic Variations ([http://www.obsebre.es/php/geomagnetisme/vrapides/ssc\\_1960\\_d.html](http://www.obsebre.es/php/geomagnetisme/vrapides/ssc_1960_d.html)). All other data are sourced from the references below.

## References

- Aa, E., Zou, S., Erickson, P. J., Zhang, S., & Liu, S. (2020). Statistical analysis of the main ionospheric trough using Swarm in situ measurements. *Journal of Geophysical Research: Space Physics*, 125, e2019Ja027583. <https://doi.org/10.1029/2019JA027583>
- Aarons, J. (1984). Equatorial trans-ionospheric propagation conditions affecting digital communications. *Paper presented at propagation influences on Digital transmission, NATO-AGARD, Electromagnetic Propagation Panel, Athens, Greece, 4–8 June* (SEE N85-19269 10-32).
- Air Navigation Order. (2019). Available at <http://www.legislation.gov.uk/uksi/2019/1115/contents/made>
- Allen, J., Frank, H., Sauer, L., & Reiff, P. (1989). Effects of the March 1989 solar activity. *Eos*, 70, 1479. <https://doi.org/10.1029/89EO00409>
- Angling, M. J., Cannon, P. S., Davies, N. C., Willink, T. J., Jodalen, V., & Lundborg, B. (1998). Measurements of Doppler and multipath spread on oblique high-latitude HF paths and their use in characterizing data modem performance. *Radio Science*, 33, 97–107. <https://doi.org/10.1029/97RS02206>
- Armstrong, T., Alsmiller, R., Jr, & Barish, J. (1969). Calculation of the radiation hazard at supersonic aircraft altitudes produced by an energetic solar flare. *Nuclear Science & Engineering*, 37, 337–342. <https://doi.org/10.13182/NSE69-A19110>
- Atkins. (2014). *Rail resilience to space weather: Final phase 1 report*. Atkins Ltd. <https://www.sparkrail.org/Lists/Records/DispForm.aspx?ID=21810>
- Bailey, D. K. (1964). Polar cap absorption, Planet. *Space Science*, 12, 495–541. [https://doi.org/10.1016/0032-0633\(64\)90040-6](https://doi.org/10.1016/0032-0633(64)90040-6)
- Bala, B., Lanzerotti, L. J., Gary, D. E., & Thomson, D. J. (2002). Noise in wireless systems produced by solar radio bursts. *Radio Science*, 37, 1018. <https://doi.org/10.1029/2001rs002481>
- Bang, E., & Lee, J. (2013). Methodology of automated ionosphere front velocity estimation for ground-based augmentation of GNSS. *Radio Science*, 48, 659–670. <https://doi.org/10.1002/rds.20066>
- Bastian, T. (2010). Radiative signatures of energetic particles. In C. J. Schrijver, & G. L. Siscoe (Eds.), *Heliophysics: Space storms and radiation: Causes and effects* (p. 79). London: Cambridge University Press. ISBN: 9780521760515.
- Basu, S., Groves, K. M., Basu, S., & Sultan, P. J. (2002). Specification and forecasting of scintillations in communication/navigation links: Current status and future plans. *Journal of Atmospheric and Solar-Terrestrial Physics*, 64, 1745–1754. [https://doi.org/10.1016/S1364-6826\(02\)00124-4](https://doi.org/10.1016/S1364-6826(02)00124-4)

## Acknowledgments

The authors of this paper are members (past and present) of the Space Environment Impacts Expert Group (SEIEG), an independent group of space weather experts that provides advice to UK government bodies. SEIEG was set up in 2010 with strong encouragement from the Civil Contingencies Secretariat (CCS), part of Cabinet Office, and, in particular, has developed and maintained the set of reasonable worst-case scenarios discussed in this paper. The authors thank the UK government bodies that have encouraged us to develop these scenarios: in particular CCS, the Government Office for Science, and the Department for Business, Energy, and Industrial Strategy. They have provided much useful guidance, as well as venues where SEIEG members could meet to progress our ideas.

M. Hapgood, M. Bisi, and R. A. Harrison acknowledge support provided by STFC, including grant ST/M001083/1. R. B. Horne was supported by NERC National Capability grants NE/R016038/1 and NE/R016445/1 and Highlight Topic Grant NE/P01738X/1 (Rad-Sat). A. W. P. Thomson acknowledges support under NERC Highlight Topic grant NE/P017231/1 (Space Weather Impact on Ground-based Systems, SWIGS). J. Eastwood acknowledges support under NERC Highlight Topics Grants NE/P017142/1 (SWIGS) and NE/P017347/1 (Rad-Sat). J. A. Wild and N. C. Rogers acknowledge support under NERC Highlight Topic grant NE/P016715/1 (SWIGS). NCR acknowledges support under NERC grant NE/V002686/1 (Space Weather Instrumentation, Measurement, Modeling and Risk, SWIMMR). C. N. Mitchell acknowledges NERC grant NE/P006450/1. The authors thank Prof. Farideh Honary for helpful discussions and support. The authors also express our thanks to Catherine Burnett for her support and encouragement of the work of SEIEG, not least this paper.

- Basu, S., MacKenzie, E., & Basu, S. (1988). Ionospheric constraints on VHF/UHF communications links during solar maximum and minimum periods. *Radio Science*, 23, 363–378. <https://doi.org/10.1029/RS023i003p00363>
- Beggan, C. D., Beamish, D., Richards, A., Kelly, G. S., & Thomson, A. W. P. (2013). Prediction of extreme geomagnetically induced currents in the UK high-voltage network. *Space Weather*, 11. <https://doi.org/10.1002/swe.20065>
- Béland, J., & Small, K. (2004). Space weather effects on power transmission systems: The cases of Hydro-Québec and Transpower New Zealand Ltd. In I. A. Daglis (Ed.), *Effects of space weather on technology infrastructure*. NATO science series II: Mathematics, physics and chemistry (Vol. 176). Dordrecht: Springer. [https://doi.org/10.1007/1-4020-2754-0\\_15](https://doi.org/10.1007/1-4020-2754-0_15)
- Boteler, D. H. (2000). Geomagnetic effects on the pipe-to-soil potentials of a Continental pipeline. *Advances in Space Research*, 26(1), 15–20. [https://doi.org/10.1016/S0273-1177\(99\)01020-0](https://doi.org/10.1016/S0273-1177(99)01020-0)
- Boteler, D. H. (2013). A new versatile method for modeling geomagnetic induction in pipelines. *Geophysical Journal International*, 193, 98–109. <https://doi.org/10.1093/gji/ggs113>
- Boteler, D. H. (2014). Methodology for simulation of geomagnetically induced currents in power systems. *Journal of Space Weather and Space Climate*, 4, A21. <https://doi.org/10.1051/swsc/2014018>
- Boteler, D. H. (2019). A 21st century view of the March 1989 magnetic storm. *Space Weather*, 17, 1427–1441. <https://doi.org/10.1029/2019SW002278>
- Boteler, D. H. (2020). Modeling geomagnetic interference on railway signaling track circuits. *Space Weather*, 18, e2020SW002609. <https://doi.org/10.1029/2020SW002609>
- Brautigam, D. H., & Bell, J. T. (1995). CRRESELE documentation, PL-TR-95-2128. Environmental research papers, 1178. Phillips Laboratory.
- Cabinet Office. (2012). *National Risk Register of Civil Emergencies* (2012 edition). [https://assets.publishing.service.gov.uk/government/uploads/system/uploads/attachment\\_data/file/211858/CO\\_NationalRiskRegister\\_2012\\_acc.pdf](https://assets.publishing.service.gov.uk/government/uploads/system/uploads/attachment_data/file/211858/CO_NationalRiskRegister_2012_acc.pdf)
- Cabinet Office. (2017). *National Risk Register of Civil Emergencies*. <https://www.gov.uk/government/collections/national-risk-register-of-civil-emergencies>
- Cabinet Office. (2019). *Sector resilience plans*. <https://www.gov.uk/government/collections/sector-resilience-plans>
- Cannon, P., Angling, M., Barclay, L., Curry, C., Dyer, C., Edwards, R., & Mitchell, C. N. (2013). *Extreme space weather: Impacts on engineered systems and infrastructure*. Royal Academy of Engineering. ISBN 1-903496-95-0 <https://www.raeng.org.uk/publications/reports/space-weather-full-report>
- Cannon, P. S. (2009). Mitigation and exploitation of the ionosphere: A military perspective. *Radio Science*, 44, RS0A20. <https://doi.org/10.1029/2008RS004021>
- Cannon, P. S., Angling, M. J., Clutterbuck, C., & Dickel, G. (2000). Measurements of the HF channel scattering function over Thailand. *Paper presented at Millenium Conference on Antennas and Propagation (AP2000), Davos, Switzerland*. Pub. ESA Publications Division, c/o ESTEC. PO Box 299, 2200 AG Noordwijk, The Netherlands.
- Cannon, P. S., Groves, K. M., Fraser, D. J., Donnelly, W. J., & Perrier, K. (2006). Signal distortion on V/UHF trans-ionospheric paths: First results from WIDE. *Radio Science*, 41, RS5S40. <https://doi.org/10.1029/2005RS003369>
- Carrano, C. S., Bridgwood, C. T., & Groves, K. M. (2009). Impacts of the December 2006 solar radio bursts on the performance of GPS. *Radio Science*, 44, RS0A25. <https://doi.org/10.1029/2008rs004071>
- Carrington, R. C. (1859). Description of a singular appearance seen in the Sun on September 1. *Monthly Notices of the Royal Astronomical Society*, 20, 13–15. <https://doi.org/10.1093/mnras/20.1.13>
- CDC (Centers for Disease Control and Prevention). (2015). *Alara – As low as reasonably achievable*. <https://www.cdc.gov/nceh/radiation/alara.html>
- Cerruti, A. P., Kintner, P. M., Gary, D. E., Mannucci, A. J., Meyer, R. F., Doherty, P., & Coster, A. J. (2008). Effect of intense December 2006 solar radio bursts on GPS receivers. *Space Weather*, 6, S10D07. <https://doi.org/10.1029/2007SW000375>
- Chapman, S. C., Horne, R. B., & Watkins, N. W. (2020). Using the aa index over the last 14 solar cycles to characterize extreme geomagnetic activity. *Geophysical Research Letters*, 47, e2019GL086524. <https://doi.org/10.1029/2019GL086524>
- Chen, G., Xu, J., Wang, W., & Burns, A. G. (2014). A comparison of the effects of CIR- and CME-induced geomagnetic activity on thermospheric densities and space-craft orbits: Statistical studies. *Journal of Geophysical Research: Space Physics*, 119, 7928–7939. <https://doi.org/10.1002/2014JA019831>
- Cid, C., Saiz, E., Guerrero, A., Palacios, J., & Cerrato, Y. (2015). A Carrington-like geomagnetic storm observed in the 21st century. *Journal of Space Weather and Space Climate*, 5, A16. <https://doi.org/10.1051/swsc/2015017>
- Claudepierre, S. G., O'Brien, T. P., Fennell, J. F., Blake, J. B., Clemmons, J. H., Looper, M. D., et al. (2017). The hidden dynamics of relativistic electrons (0.7–1.5 MeV) in the inner zone and slot region. *Journal of Geophysical Research: Space Physics*, 122, 3127–3144. <https://doi.org/10.1002/2016JA023719>
- Claudepierre, S. G., O'Brien, T. P., Looper, M. D., Blake, J. B., Fennell, J. F., Roeder, J. L., et al. (2019). A revised look at relativistic electrons in the Earth's inner radiation zone and slot region. *Journal of Geophysical Research: Space Physics*, 124, 934–951. <https://doi.org/10.1029/2018JA026349>
- Cliver, E. W., & Dietrich, W. F. (2013). The 1859 space weather event revisited: Limits of extreme activity. *Journal of Space Weather and Space Climate*, 3, A31. <https://doi.org/10.1051/swsc/2013053>
- Cliver, E. W., & Svalgaard, L. (2004). The 1859 solar-terrestrial disturbance and the current limits of extreme space weather activity. *Solar Physics*, 224, 407–422. <https://doi.org/10.1007/s11207-005-4980-z>
- Conker, R. S., El-Arini, M. B., Hegarty, C. J., & Hsiao, T. (2003). Modeling the effects of ionospheric scintillation on GPS/Satellite-Based Augmentation System availability. *Radio Science*, 38, 1001. <https://doi.org/10.1029/2000RS002604>
- Datta-Barua, S., Lee, J., Pullen, S., Luo, M., Ene, A., Qiu, D., & Enge, P. (2010). Ionospheric threat parameterization for local area global-positioning-system-based aircraft landing systems. *Journal of Aircraft*, 47, 1141–1151. <https://doi.org/10.2514/1.46719>
- Davies, K. (1990). Ionospheric radio. In *IEE electromagnetic waves series* (Vol. 31). London: Peter Peregrinus Ltd. on behalf of the Institution of Electrical Engineers.
- De Franceschi, G., Alfonsi, L., Romano, V., Aquino, M., Dodson, A., Mitchell, C. N., & Wernik, A. W. (2008). Dynamics of high-latitude patches and associated small-scale irregularities during the October and November 2003 storms. *Journal of Atmospheric and Solar-Terrestrial Physics*, 70, 879–888. <https://doi.org/10.1016/j.jastp.2007.05.018>
- Deutsch, M.-J. C. (1982). Worst case earth charging environment. *Journal of Spacecraft*, 19, 82–4223. <https://doi.org/10.2514/3.62287>
- Drury, J., Novelli, D., & Stott, C. (2013). Representing crowd behavior in emergency planning guidance: 'mass panic' or collective resilience?. *Resilience*, 1(1), 18–37. <https://doi.org/10.1080/21693293.2013.765740>
- Duggal, S. P. (1979). Relativistic solar cosmic rays. *Reviews of Geophysics*, 17, 1021–1058. <https://doi.org/10.1029/RG017i005p01021>

- Dyer, A., Hands, A., Ryden, K., Dyer, C., Flintoff, I., & Ruffenach, A. (2020). Single event effects in ground level infrastructure during extreme ground level enhancements. *IEEE Transactions on Nuclear Science*, 67, 1139–1143. <https://doi.org/10.1109/TNS.2020.2975838>
- Dyer, C., Hands, A., Ryden, K., & Lei, F. (2017). Extreme atmospheric radiation environments & single event effects. *IEEE Transactions on Nuclear Science*, 65, 432–438. <https://doi.org/10.1109/TNS.2017.2761258>
- Dyer, C. S., Lei, F., Clucas, S. N., Smart, D. F., & Shea, M. A. (2003). Solar particle enhancements of single event effect rates at aircraft altitudes. *IEEE Transactions on Nuclear Science*, 50, 2038–2045. <https://doi.org/10.1109/TNS.2003.821375>
- Dyer, C. S., Lei, F., Hands, A., & Truscott, P. (2007). Solar particle events in the QinetiQ atmospheric radiation model. *IEEE Transactions on Nuclear Science*, 54, 1071–1075. <https://doi.org/10.1109/TNS.2007.893537>
- Dyer, C. S., Sims, A. J., Farren, J., & Stephen, J. (1989). Measurements of the SEU environment in the upper atmosphere. *IEEE Transactions on Nuclear Science*, 36, 2275–2280. <https://doi.org/10.1109/23.45435>
- Eastwood, J. (2008). The science of space weather. *Philosophical Transactions of the Royal Society*, 366, 4489–4500. <https://doi.org/10.1098/rsta.2008.016>
- Eastwood, J. P., Hapgood, M. A., Biffis, E., Benedetti, D., Bisi, M. M., Green, L., et al. (2018). Quantifying the economic value of space weather forecasting for power grids: An exploratory study. *Space Weather*, 16, 2052–2067. <https://doi.org/10.1029/2018SW002003>
- ECSS. (2008). *European cooperation for space standardization*. ECSS-E-ST-10-04C: Space engineering – Space environment. Retrieved from <http://www.ecss.nl/>
- Elvidge, S. (2020). Estimating the occurrence of geomagnetic activity using the Hilbert-Huang transform and extreme value theory. *Space Weather*, 18, e2020SW002513. <https://doi.org/10.1029/2020SW002513>
- Elvidge, S., & Angling, M. J. (2018). Using extreme value theory for determining the probability of Carrington-like solar flares. *Space Weather*, 16, 417–421. <https://doi.org/10.1002/2017SW001727>
- Erinmez, I. A., Kappenman, J. G., & Radasky, W. A. (2002). Management of the geomagnetically induced current risks on the National Grid Company's electric power transmission system. *Journal of Atmospheric and Solar-Terrestrial Physics*, 64, 743–756. [https://doi.org/10.1016/S1364-6826\(02\)00036-6](https://doi.org/10.1016/S1364-6826(02)00036-6)
- Eroshenko, E. A., Belov, A. V., Boteler, D. H., Gaidash, S. P., & Lobkov, S. L. (2010). Effects of strong geomagnetic storms on Northern railways in Russia. *Advances in Space Research*, 46, 1102–1110. <https://doi.org/10.1016/j.asr.2010.05.017>
- EURATOM. (1996). Council Directive 96/29/Euratom of 13 May 1996, "Laying down basic safety standards for the protection of the health of workers and the general public against the dangers arising from ionizing radiation". *Official Journal of the European Communities*, L159, 1–114. <http://data.europa.eu/eli/dir/1996/29/oj>
- EURATOM (2013). Council Directive 2013/59/Euratom of 5 December 2013. Laying down basic safety standards for protection against the dangers arising from exposure to ionising radiation. *Official Journal of the European Union L 013*, 2014. <https://eur-lex.europa.eu/eli/dir/2013/59/oj>
- Fennell, J. F., Claudepierre, S. G., Blake, J. B., O'Brien, T. P., Clemmons, J. H., Baker, D. N., et al. (2015). Van Allen Probes show that the inner radiation zone contains no MeV electrons: ECT/MagEIS data. *Geophysical Research Letters*, 42, 1283–1289. <https://doi.org/10.1002/2014GL062874>
- Fennell, J. F., Koons, H. C., Roeder, J. L., & Blake, J. B. (2001). *Spacecraft charging: Observations and relationship to satellite anomalies*. Aerospace Report TR-2001 8570-5. <http://www.dtic.mil/cgi-bin/GetTRDoc?AD=ADA394826>
- Foelsche, T. (1962). *Radiation exposure in supersonic transports*, Technical Note D-1383. National Aeronautics and Space Administration <https://ntrs.nasa.gov/search.jsp?R=19620005014>
- Foelsche, T. (1964). *The ionizing radiations in supersonic transport flights*. Technical Memorandum X-56122. <https://ntrs.nasa.gov/search.jsp?R=19650009320>
- Forbush, S. E. (1946). Three unusual cosmic-ray increases possibly due to charged particles from the Sun. *Physical Review*, 70, 771. <https://doi.org/10.1103/PhysRev.70.771>
- Franke, E. (1996). Effects of solar, Galactic and man-made noise on UHF SATCOM operation. Proceedings of MILCOM'96 IEEE military communications Conference (Vol. 1, pp. 29–36). IEEE. <https://doi.org/10.1109/MILCOM.1996.568578>
- Gaunt, C. T. (2014). Reducing uncertainty – Responses for electricity utilities to severe solar storms. *Journal of Space Weather and Space Climate*, 4, A01. <https://doi.org/10.1051/swsc/2013058>
- Ginet, G. P., O'Brien, T. P., Huston, S. L., Johnston, W. R., Guild, T. B., Friedel, R., & Madden, D. (2013). AE9, AP9 and SPM: New models for specifying the trapped energetic particle and space plasma environment. *Space Science Reviews*, 179, 579–615. <https://doi.org/10.1007/s11214-013-9964-y>
- Gombosi, T. I., Baker, D. N., Balogh, A., Erickson, P. J., Huba, J. D., & Lanzerotti, L. J. (2017). Anthropogenic space weather. *Space Science Reviews*, 212, 985–1039. <https://doi.org/10.1007/s11214-017-0357-5>
- Gopalswamy, N. (2018). Extreme solar eruptions and their space weather consequences. In N. Buzulukova (Ed.), *Extreme events in the Geospace* (pp. 37–63). Elsevier. <https://doi.org/10.1016/B978-0-12-812700-1.00002-9>
- Green, J. L., & Boardsen, S. (2006). Duration and extent of the great auroral storm of 1859. *Advances in Space Research*, 38, 130–135. <https://doi.org/10.1016/j.asr.2005.08.054>
- Gummow, R. A. (2002). GIC effects on pipeline corrosion and corrosion control systems. *Journal of Atmospheric and Solar-Terrestrial Physics*, 64, 1755–1764. [https://doi.org/10.1016/S1364-6826\(02\)00125-6](https://doi.org/10.1016/S1364-6826(02)00125-6)
- Gussenhoven, M. S., & Mullen, E. G. (1983). Geosynchronous environment for severe spacecraft charging. *Journal of Spacecraft and Rockets*, 20, 26. <https://doi.org/10.2514/3.28353>
- Hands, A. D. P., Ryden, K. A., Meredith, N. P., Glauert, S. A., & Horne, R. B. (2018). Radiation effects on satellites during extreme space weather events. *Space Weather*, 16, 1216–1226. <https://doi.org/10.1029/2018SW001913>
- Hapgood, M. (2018). Space weather: What are Policymakers seeking?. In N. Buzulukova (Ed.), *Extreme events in Geospace* (pp. 657–682). Elsevier. <https://doi.org/10.1016/B978-0-12-812700-1.00027-3>
- Hapgood, M. (2019a). The great storm of May 1921: An exemplar of a dangerous space weather event. *Space Weather*, 17, 950–975. <https://doi.org/10.1029/2019SW002195>
- Hapgood, M. (2019b). Technological impacts of space weather. In *Geomagnetism, aeronomy and space weather: A journey from the Earth's core to the Sun*. Cambridge University Press. <https://doi.org/10.1017/9781108290135.01>
- Hapgood, M., Angling, M., Attrill, G., Bisi, M., Burnett, C., Cannon, P., et al. (2020). *Summary of space weather worst-case environments*. RAL Technical Report RAL-TR-2020-005 (Second revised edition). <https://epubs.stfc.ac.uk/work/46642513>
- Hapgood, M., Angling, M., Attrill, G., Burnett, C., Cannon, P., Gibbs, M., et al. (2016). *Summary of space weather worst-case environments*. RAL Technical Report RAL-TR-2016-006 (Revised edition). <https://epubs.stfc.ac.uk/work/25015281>

- Hapgood, M., Horne, R., Kerridge, D., Jones, B., Cannon, P., Ryden, K., et al. (2012). *Summary of space weather worst-case environments*. RAL Technical Report RAL-TR-2012-022. <https://epubs.stfc.ac.uk/work/64253>
- Hapgood, M. A. (2011). Toward a scientific understanding of the risk from extreme space weather. *Advances in Space Research*, 47(12), 2059–2072. <https://doi.org/10.1016/j.asr.2010.02.007>
- Hartz, T. R., & Brice, N. M. (1967). The general pattern of auroral particle precipitation. *Planetary and Space Science*, 15, 301–329. [https://doi.org/10.1016/0032-0633\(67\)90197-3](https://doi.org/10.1016/0032-0633(67)90197-3)
- Haug, E. G. (2010). *When will God destroy our money?*. Available at SSRN: <https://doi.org/10.2139/ssrn.1591768>
- Hayakawa, H., Iwahashi, K., Ebihara, Y., Tamazawa, H., Shibata, K., Knipp, D. J., et al. (2017). Long-lasting extreme magnetic storm activities in 1770 found in historical documents. *Acta Pathologica Japonica*, 850, L31. <https://doi.org/10.3847/2041-8213/aa9661>
- Hey, J. S. (1946). Solar radiations in the 4–6 meter radio wave-length band. *Nature*, 157, 47–48. <https://doi.org/10.1038/157047b0>
- Hodgson, R. (1859). On a curious appearance seen in the Sun. *Monthly Notices of the Royal Astronomical Society*, 20, 15–16. <https://doi.org/10.1093/mnras/20.1.15>
- Horne, R. B., Phillips, M. W., Glauert, S. A., Meredith, N. P., Hands, A. D. P., Ryden, K., & Li, W. (2018). Realistic worst case for a severe space weather event driven by a fast solar wind stream. *Space Weather*, 16, 1202–1215. <https://doi.org/10.1029/2018SW001948>
- Horne, R. B., & Pitchford, D. (2015). Space weather concerns for all-electric propulsion satellites. *Space Weather*, 13, 430–433. <https://doi.org/10.1002/2015SW001198>
- Horne, R. B., Thorne, R. M., Shprits, Y. Y., Meredith, N. P., Glauert, S. A., Smith, A. J., et al. (2005). Wave acceleration of electrons in the Van Allen radiation belts. *Nature*, 437, 227–230. <https://doi.org/10.1038/nature03939>
- House of Lords Science and Technology Committee. (2005). *Pandemic influenza: Report with evidence*. London: HMSO, 124
- HSE (Health and Safety Executive). (1992). *The tolerability of risk from nuclear power stations*. <http://www.onr.gov.uk/documents/tolerability.pdf>
- Hunsucker, R. D., & Hargreaves, J. K. (2003). *The high-latitude ionosphere and its effects on radio propagation*. Cambridge University Press. ISBN 0 521 33083 1.
- ICAO. (2018). *International standards and recommended practices. Annex 3 to the Convention on International Civil Aviation, Meteorological Service for International Air Navigation* (20th ed.). ISBN 978-92-9258-482-5.
- ICAO. (2019). *ICAO manual on space weather information in support of international air navigation* (1st ed.). ICAO Doc 10100. ISBN 978-92-9258-662-1.
- ICRP. (1977). *Recommendations of the International Commission on Radiological Protection*. Publication 26. Annals of the ICRP, 1.
- ICRP. (1991). *1990 recommendations of the International Commission on Radiological Protection*. Publication 60. Annals of the ICRP.
- ICRP. (2007). *Recommendations of the International Commission on Radiological Protection*. Publication 103. *Annals of the ICRP*, 37, 2–4.
- ICRP. (2016). *Radiological protection from cosmic radiation in aviation*. ICRP Publication 132. *Annals of the ICRP*, 45, 1–48.
- IEC. (2016). *Process management for avionics: Atmospheric radiation effects. Part 1: Accommodation of atmospheric radiation effects via single event effects within avionics electronic equipment* (2nd ed.). *International Electrotechnical Commission document*. 62396-1:2016.
- IEC. (2017). *Process management for avionics: Atmospheric radiation effects. Part 6: Extreme space weather—Potential impact on the avionics environment and electronics* (1st ed.). *International Electrotechnical Commission document*. 62396-6:2017.
- Ingham, M., & Rodger, C. J. (2018). Telluric field variations as drivers of variations in cathodic protection potential on a natural gas pipeline in New Zealand. *Space Weather*, 16, 1396–1409. <https://doi.org/10.1029/2018SW001985>
- JEDEC (2006). *Measurement and reporting of alpha particle and terrestrial cosmic ray-induced soft errors in semiconductor devices*. In *Joint Electron Device Engineering Council (JEDEC) standard JESD89A*. <https://www.jedec.org/standards-documents/docs/jesd-89a>
- Jonas, S., Fronczyk, K., & Pratt, L. M. (2018). A framework to understand extreme space weather event probability. *Risk Analysis*, 38, 1534–1540. <https://doi.org/10.1111/risa.12981>
- Kappenman, J. G. (2006). Great geomagnetic storms and extreme impulsive geomagnetic field disturbance events – An analysis of observational evidence including the great storm of May 1921. *Advances in Space Research*, 38, 188–199. <https://doi.org/10.1016/j.asr.2005.08.055>
- Karpachev, A. T., Klimenko, M. V., Klimenko, V. V., & Pustovalova, L. V. (2016). Empirical model of the main ionospheric trough for the nighttime winter conditions. *Journal of Atmospheric and Solar-Terrestrial Physics*, 146, 149–159. <https://doi.org/10.1016/j.jastp.2016.05.008>
- Kataoka, R., & Iwahashi, K. (2017). Inclined zenith aurora over Kyoto on 17 September 1770: Graphical evidence of extreme magnetic storm. *Space Weather*, 15, 1314–1320. <https://doi.org/10.1002/2017SW001690>
- Kelly, G. S., Viljanen, A., Beggan, C. D., & Thomson, A. W. P. (2017). Understanding GIC in the UK and French high-voltage transmission systems during severe magnetic storms. *Space Weather*, 15, 99–114. <https://doi.org/10.1002/2016SW001469>
- Kerr, R. (2011). Into the stretch for science's point man on Doomsday. *Science*, 6045(333), 929–929. <https://doi.org/10.1126/science.333.6045.928>
- Kintner, P. M., Coster, A. J., Fuller-Rowell, T., Mannucci, A. J., Mendillo, M., & Heelis, R. (2013). Midlatitude ionospheric dynamics and disturbances. *Geophysical Monograph*, 181. <https://doi.org/10.1029/GM181>
- Kintner, P. M., Ledvina, B. M., & de Paula, E. R. (2007). GPS and ionospheric scintillations. *Space Weather*, 5, S09003. <https://doi.org/10.1029/2006SW000260>
- Knipp, D. J., Fraser, B. J., Shea, M. A., & Smart, D. F. (2018). On the little-known consequences of the 4 August 1972 ultra-fast coronal mass ejecta: Facts, commentary, and call to action. *Space Weather*, 16, 1635–1643. <https://doi.org/10.1029/2018SW002024>
- Knipp, D. J., Pette, D. V., Kilcommons, L. M., Isaacs, T. L., Cruz, A. A., Mlynczak, M. G., et al. (2017). Thermospheric nitric oxide response to shock-led storms. *Space Weather*, 15, 325–342. <https://doi.org/10.1002/2016SW001567>
- Koons, H. C. (2001). Statistical analysis of extreme values in space science. *Journal of Geophysical Research*, 106, 10915–10921. <https://doi.org/10.1029/2000JA000234>
- Krausmann, E., Andersson, E., Russell, T., & Murtagh, W. (2015). *Space weather and rail: Outlook and finding, 16–17 September 2015*. Publications Office of the European Union. <https://doi.org/10.2788/211456>
- Krauss, S., Temmer, M., & Vennerstrom, S. (2018). Multiple satellite analysis of the Earth's thermosphere and interplanetary magnetic field variations due to ICME/CIR events during 2003–2015. *Journal of Geophysical Research*, 123, 8884–8894. <https://doi.org/10.1029/2018JA025778>
- Krauss, S., Temmer, M., Veronig, A., Baur, O., & Lammer, H. (2015). Thermospheric and geomagnetic responses to interplanetary coronal mass ejections observed by ACE and GRACE: Statistical results. *Journal of Geophysical Research*, 120, 8848–8860. <https://doi.org/10.1002/2015JA021702>

- Lanzerotti, L. J., Thomson, D. J., & MacLennan, C. G. (1999). Engineering issues in space weather. In M. A. Stuchly (Ed.), *Modern radio science 1999* (pp. 25–50). Hoboken, NJ: John Wiley. ISBN 9780780360020.
- Le, H., Liu, L., Ren, Z., ChenZhang, Y. H., & Wan, W. (2016). A modeling study of global ionospheric and thermospheric responses to extreme solarflare. *Journal of Geophysical Research: Space Physics*, *121*, 832–840. <https://doi.org/10.1002/2015JA021930>
- Love, J. J. (2012). Credible occurrence probabilities for extreme geophysical events: Earthquakes, volcanic eruptions, magnetic storms. *Geophysical Research Letters*, *39*, L10301. <https://doi.org/10.1029/2012GL051431>
- Love, J. J., Hayakawa, H., & Cliver, E. W. (2019). Intensity and impact of the New York Railroad superstorm of May 1921. *Space Weather*, *17*, 1281–1292. <https://doi.org/10.1029/2019SW002250>
- Mannucci, A. J., Tsurutani, B. T., Iijima, B. A., Komjathy, A., SaitoGonzalez, A. W. D., Guarnieri, F. L., et al. (2005). Dayside global ionospheric response to the major interplanetary events of October 29–30, 2003 “Halloween Storms”. *Geophysical Research Letters*, *32*, L12S02. <https://doi.org/10.1029/2004GL021467>
- Marqué, C., Klein, K. L., Monstein, C., Opgenoorth, H., Pulkkinen, A., Buchert, S., et al. (2018). Solar radio emission as a disturbance of aeronautical radionavigation. *Journal of Space Weather and Space Climate*, *8*, A42. <https://doi.org/10.1051/swsc/2018029>
- Matéo-Vélez, J. -C., Sicard, A., Payan, D., Ganushkina, N., Meredith, N. P., & Sillanpää, I. (2018). Spacecraft surface charging induced by severe environments at geosynchronous orbit. *Space Weather*, *16*, 89–106. <https://doi.org/10.1002/2017SW001689>
- Matsushita, S. (1959). A study of the morphology of ionospheric storms. *Journal of Geophysical Research*, *64*, 305. <https://doi.org/10.1029/JZ064i003p00305>
- McBeath, A. (1999). Meteors, comets and millennialism. *Journal of the IMO*, *27*, 318–326. Available on ADS with bibliographic code: 1999JIMO...27.318M.
- McCracken, K., Shea, M. A., & Smart, D. (2016). The short-lived (< 2 minutes) acceleration of protons to > 13 GeV in association with solar flares. EGU general Assembly Conference Abstracts (Vol. 18, p. 9634).
- McCracken, K. G., & Beer, J. (2015). The annual cosmic-radiation intensities 1391–2014; the annual heliospheric magnetic field strengths 1391–1983, and identification of solar cosmic-ray events in the cosmogenic record 1800–1983. *Solar Physics*, *290*, 3051–3069. <https://doi.org/10.1007/s11207-015-0777-x>
- McCracken, K. G., Moraal, H., & Shea, M. A. (2012). The high-energy impulsive ground-level enhancement. *Acta Pathologica Japonica*, *76*(1), 101. <https://doi.org/10.1088/0004-637X/761/2/101>
- McCrone, P. R., Dhanasiri, S., Patel, A., Knapp, M., & Lawton-Smith, S. (2008). *Paying the price: The cost of mental health care in England to 2026*. King’s Fund. <https://www.kingsfund.org.uk/publications/paying-price>
- McIlwain, C. E. (1961). Coordinates for mapping the distribution of magnetically trapped particles. *Journal of Geophysical Research*, *66*, 3681–3691. <https://doi.org/10.1029/JZ066i011p03681>
- Mekhaldi, F., Muscheler, R., Adolphi, F., Aldahan, A., Beer, J., McConnell, J. R., et al. (2015). Multiradionuclide evidence for the solar origin of the cosmic-ray events of AD 774/5 and 993/4. *Nature Communications*, *6*. <https://doi.org/10.1038/ncomms9611>
- Meredith, N. P., Horne, R. B., Isles, J. D., & Green, J. C. (2016). Extreme energetic electron fluxes in low Earth orbit: Analysis of POES E > 30, E > 100 and E > 300 keV electrons. *Space Weather*, *14*, 136–150. <https://doi.org/10.1002/2015SW001348>
- Meredith, N. P., Horne, R. B., Isles, J. D., & Rodriguez, J. V. (2015). Extreme relativistic electron fluxes at geosynchronous orbit: Analysis of GOES E > 2 MeV electrons. *Space Weather*, *13*. <https://doi.org/10.1002/2014SW001143>
- Meredith, N., Horne, R., Isles, J., Ryden, K., Hands, A., & Heynderickx, D. (2016). Extreme internal charging currents in medium Earth orbit: Analysis of SURF plate currents on Giove-A. *Space Weather*, *14*, 578–591. <https://doi.org/10.1002/2016SW001404>
- Meredith, N. P., Horne, R. B., Sandberg, I., Papadimitriou, C., & Evans, H. D. R. (2017). Extreme relativistic electron fluxes in the Earth’s outer radiation belt: Analysis of INTEGRAL IREM data. *Space Weather*, *15*, 917–933. <https://doi.org/10.1002/2017SW001651>
- Miyake, F., Nagaya, K., Masuda, K., & Nakamura, T. (2012). A signature of cosmic-ray increase in AD 774–775 from tree rings in Japan. *Nature*, *486*, 240–242. <https://doi.org/10.1038/nature11123>
- Miyake, F., Usoskin, I., Poluianov, S., et al. (2020). *Extreme solar particle events: The hostile Sun*. Bristol: IOP Publishing Ltd. <https://doi.org/10.1088/2514-3433/ab404a>
- Mullen, E. G., Gussenhoven, M. S., & Garrett, H. B. (1981). A ‘worst case’ spacecraft charging environment as observed by, SCATHA on 24 April 1979. *AFGL-TR-81-0231*. <https://apps.dtic.mil/dtic/tr/fulltext/u2/a108680.pdf>
- NASA. (2017). *Mitigating in-space charging effects-A Guideline*. NASA-HDBK-4002. <https://standards.nasa.gov/standard/oc/nasa-hdbk-4002>
- National Science and Technology Council. (2018). Space weather phase 1 benchmarks. In *National science and technology (US) Space Weather Operations, Research and Mitigation subcommittee*. Washington, DC: Executive Office of the President of the United States.
- Nava, B., Coisson, P., & Radicella, S. (2008). A new version of the NeQuick ionosphere electron density model. *Journal of Atmospheric and Solar-Terrestrial Physics*, *70*, 1856–1862. <https://doi.org/10.1016/j.jastp.2008.01.015>
- Ngwira, C. M., Pulkkinen, A., Wilder, F. D., & Crowley, G. (2013). Extended study of extreme geoelectric field event scenarios for geomagnetically induced current applications. *Space Weather*, *11*, 121–131. <https://doi.org/10.1002/swe.20021>
- Ngwira, C. M., Pulkkinen, A. A., Bernabeu, E., Eichner, J., Viljanen, A., & Crowley, G. G. (2015). Characteristics of extreme geoelectric fields and their possible causes: Localized peak enhancements. *Geophysical Research Letters*, *42*, 6916–6921. <https://doi.org/10.1002/2015GL065061>
- NOAA. (1960). *Solar-geophysical data, December 1960*. CRPL-F 196. Part B. ftp://ftp.ngdc.noaa.gov/STP/SOLAR\_DATA/SGD\_PDFversion/1960/sgd6012.pdf
- NOAA. (1961). *Solar-geophysical data, January 1961*. CRPL-F 197. Part B. ftp://ftp.ngdc.noaa.gov/STP/SOLAR\_DATA/SGD\_PDFversion/1961/sgd6101.pdf
- Normand, E. (1996). Single event upset at ground level. *IEEE Transactions on Nuclear Science*, *43*, 2742–2750. <https://doi.org/10.1109/23.556861>
- NSTB/WAAS Test and Evaluation Team. (2004). Wide-area augmentation system performance analysis report. *Tech. Rep. 7*, William J. Hughes Tech. Cent., fed. Aviation Admin, Atlantic City, NJ.
- O’Hare, P., Mekhaldi, F., Adolphi, F., Raisbeck, G., Aldahan, A., Anderberg, E., et al. (2019). Multiradionuclide evidence for an extreme solar proton event around 2,610 BP (~ 660 BC). *Proceedings of the National Academy of Sciences*, *116*, 5961–5966. <https://doi.org/10.1073/pnas.1815725116>
- Oliveira, D. M., Zesta, E., Schuck, P. W., & Sutton, E. K. (2017). Thermosphere global time response to geomagnetic storms caused by coronal mass ejections. *Journal of Geophysical Research: Space Physics*, *122*, 10762–10782. <https://doi.org/10.1002/2017JA024006>

- Oughton, E. J., Hapgood, M., Richardson, G. S., Beggan, C. D., Thomson, A. W. P., et al. (2019). A risk assessment framework for the Socioeconomic impacts of electricity transmission infrastructure failure due to space weather: An application to the United Kingdom. *Risk Analysis*, 39, 1022–1043. <https://doi.org/10.1111/risa.13229>
- Oxford Economics. (2010). *The economic impacts of air travel restrictions due to volcanic ash*. <https://www.oxfordeconomics.com/my-oxford/projects/129051>
- Palmer, J. (2016). Purity and Danger in the solar Temple. In J. Lewis (Ed.), *The Order of the Solar Temple: The Temple of Death* (pp. 39–55). London: Routledge. ISBN 978-0-7546-5284-4.
- Parthasarathy, R., Lerfald, G. M., & Little, C. G. (1963). Derivation of electron density profiles in the lower ionosphere using radio absorption measurements at multiple frequencies. *Journal of Geophysical Research*, 68, 3581–3588. <https://doi.org/10.1029/JZ068i012p03581>
- Preston, J., Chadderton, C., Kaori, K., & Edmonds, C. (2015). Community response in disasters: An ecological learning framework. *International Journal of Lifelong Education*, 34, 727–753. <https://doi.org/10.1080/02601370.2015.1116116>
- Pulkkinen, A., Bernabeu, E., Eichner, J., Viljanen, A., & Ngwira, C. (2015). Regional-scale high-latitude extreme geoelectric fields pertaining to geomagnetically induced currents. *Earth, Planets and Space*, 67, 93. <https://doi.org/10.1186/s40623-015-0255-6>
- Pulkkinen, A., Bernabeu, E., Thomson, A., Viljanen, A., Pirjola, R., Boteler, D., et al. (2017). Geomagnetically induced currents: Science, engineering, and applications readiness. *Space Weather*, 15, (7), 828–856. <http://dx.doi.org/10.1002/2016sw001501>
- Reames, D. V. (1999). Particle acceleration at the Sun and in the heliosphere. *Space Science Reviews*, 90, 413. <https://doi.org/10.1023/A:1005105831781>
- Redmon, R. J., Seaton, D. B., Steenburgh, R., He, J., & Rodriguez, J. V. (2018). September 2017's geoeffective space weather and impacts to Caribbean radio communications during hurricane response. *Space Weather*, 16, 1190–1201. <https://doi.org/10.1029/2018SW001897>
- Reeves, G., Colvin, T., Locke, J., et al (2019). *Next steps space weather benchmarks*. IDA Group Report NS GR-10982. Washington, DC: Institute for Defense Analyses. December 2019. <https://www.ida.org/research-and-publications/publications/all/n/ne/next-step-space-weather-benchmarks>
- Riley, P. (2012). On the probability of occurrence of extreme space weather events. *Space Weather*, 10, S02012. <https://doi.org/10.1029/2011SW000734>
- Riley, P., & Love, J. J. (2017). Extreme geomagnetic storms: Probabilistic forecasts and their uncertainties. *Space Weather*, 15, 53–64. <https://doi.org/10.1002/2016SW001470>
- Rishbeth, H., Shea, M. A., & Smart, D. F. (2009). The solar-terrestrial event of 23 February 1956. *Advances in Space Research*, 44, 1096–1106. <https://doi.org/10.1016/j.asr.2009.06.020>
- Roederer, J. G. (1970). *Dynamics of geomagnetically trapped radiation*. New York, NY: Springer. <https://doi.org/10.1007/978-3-642-49300-3>
- Roederer, J. G., & Lejosne, S. (2018). Coordinates for representing radiation belt particle flux. *Journal of Geophysical Research: Space Physics*, 123, 1381–1387. <https://doi.org/10.1002/2017JA02505>
- Rogers, N. C., Wild, J. A., Eastoe, E. F., Gjerloev, J. W., & Thomson, A. W. P. (2020). A global climatological model of extreme geomagnetic field fluctuations. *Journal of Space Weather and Space Climate*, 10, 5. <https://doi.org/10.1051/swsc/2020008>
- Ryden, K. (2018). *The in-situ measurement of spacecraft internal charging currents*. Doctoral dissertation, University of Surrey. [https://eprints.surrey.ac.uk/849794/7/KARyden\\_PhD\\_Thesis\\_Oct\\_2018\\_Part1.pdf](https://eprints.surrey.ac.uk/849794/7/KARyden_PhD_Thesis_Oct_2018_Part1.pdf)
- Sauer, H. H., & Wilkinson, D. C. (2008). Global mapping of ionospheric HF/VHF radio wave absorption due to solar energetic protons. *Space Weather*, 6, S12002. <https://doi.org/10.1029/2008SW000399>
- Sciencewise (2015). *Space weather public dialogue: Summary and final report*. <http://webarchive.nationalarchives.gov.uk/20180103171136/http://www.sciencewise-erc.org.uk/cms/space-weather-dialogue/>
- Shea, M. A., & Smart, D. F. (2000). Fifty years of cosmic radiation data. *Space Science Reviews*, 93, 229–262. <https://doi.org/10.1023/A:1026500713452>
- Shprits, Y., Subbotin, D., Ni, B., Horne, R., Baker, D., & Cruce, P. (2011). Profound change of the near-Earth radiation environment caused by solar superstorms. *Space Weather*, 9, S08007. <https://doi.org/10.1029/2011SW000662>
- Simpson, J. A. (2000). The cosmic ray nucleonic component: The invention and scientific Uses of the neutron monitor (Keynote Lecture). *Space Science Reviews*, 93, 11–32. <https://doi.org/10.1023/A:1026567706183>
- Smith, R. (2006). Hurricane force. *Physics World*, 19(6), 32–37. <https://doi.org/10.1088/2058-7058/19/6/35>
- SPENVIS. (2018). *McIlwain's (B,L) coordinate system*. <https://www.spennis.oma.be/help/background/magfield/bl.html>
- Stenquist, D. (1925). *Etude des courants telluriques, Mémoires publiés par la Direction Générale des Télégraphes de Suède*. Stockholm (printed by R.W. Statlanders boktryckeri).
- Sutton, E. K., Forbes, J. M., & Knipp, D. J. (2009). Rapid response of the thermosphere to variations in Joule heating. *Journal of Geophysical Research*, 114, A04319. <https://doi.org/10.1029/2008JA013667>
- Sutton, E. K., Forbes, J. M., & Nerem, R. S. (2005). Global thermospheric neutral density and wind response to the severe 2003 geomagnetic storms from CHAMP accelerometer data. *Journal of Geophysical Research*, 110, A09S40. <https://doi.org/10.1029/2004JA010985>
- Thomson, A. W. P., Dawson, E. B., & Reay, S. J. (2011). Quantifying extreme behavior in geomagnetic activity. *Space Weather*, 9, S10001. <https://doi.org/10.1029/2011SW000696>
- Thomson, A. W. P., McKay, A. J., Clarke, E., & Reay, S. J. (2005). Surface electric fields and geomagnetically induced currents in the Scottish Power grid during the 30 October 2003 geomagnetic storm. *Space Weather*, 3, S11002. <https://doi.org/10.1029/2005SW000156>
- Thomson, N. R., Rodger, C. J., & Dowden, R. L. (2004). Ionosphere gives size of greatest solar flare. *Geophysical Research Letters*, 31, L06803. <https://doi.org/10.1029/2003GL019345>
- Tylka, A. J., Adams, J. H., Boberg, P. R., Brownstein, B., Dietrich, W. F., Flueckiger, E. O., & Smith, E. C. (1997). CREME96: A revision of the cosmic ray effects on micro-electronics code. *IEEE Transactions on Nuclear Science*, 44(6), 2150–2160. <https://doi.org/10.1109/23.659030>
- Tylka, A. J., & Dietrich, W. (2009). A new and comprehensive analysis of proton spectra in ground-level enhanced (GLE) solar particle events. *Proceedings of the 31st International Cosmic Ray Conference (Łódź)* (pp. 7–15).
- Usoskin, I. G., & Kovaltsov, G. A. (2012). Occurrence of extreme solar particle events: assessment from historical proxy data. *The Astrophysical Journal*, 757(1), 92. <http://dx.doi.org/10.1088/0004-637x/757/1/92>
- Vette, J. I. (1991). *The AE-8 trapped electron model environment*. NASA report NSSDC/WDC-A-R&S 91-24 <https://ntrs.nasa.gov/search.jsp?R=19920014985>
- Warrington, E. M., Rogers, N. C., & Jones, T. B. (1997). Large HF bearing errors for propagation paths contained within the polar cap. *IEE Proceedings – Microwaves, Antennas and Propagation*, 144, 241–249. <https://doi.org/10.1049/ip-map:19971187>
- Weber, E. J., Buchau, J., Moore, J. G., Sharber, J. R., Livingston, R. C., Winningham, J. D., & Reinisch, B. W. (1984). F layer ionization patches in the polar cap. *Journal of Geophysical Research*, 89, 1683–1694. <https://doi.org/10.1029/JA089iA03p01683>

- West, H. I., Jr. & Buck, R. M. (1976a). A study of electron spectra in the inner belt. *Journal of Geophysical Research*, *81*, 4696–4700. <https://doi.org/10.1029/JA081i025p04696>
- West, H. I., Jr. & Buck, R. M. (1976b). Energetic electrons in the inner belt in 1968. *Planetary and Space Science*, *24*, 643–655. [https://doi.org/10.1016/0032-0633\(76\)90032-5](https://doi.org/10.1016/0032-0633(76)90032-5)
- Wik, M., Pirjola, R., Lundstedt, H., Viljanen, A., Wintoft, P., & Pulkkinen, A. (2009). Space weather events in July 1982 and October 2003 and the effects of geomagnetically induced currents on Swedish technical systems. *Annales Geophysicae*, *27*, 1775–1787. <https://doi.org/10.5194/angeo-27-1775-2009>
- Xapsos, M. A., Summers, G. P., Barth, J. L., Stassinopoulos, E. G., & Burke, E. A. (1999). Probability model for worst case solar proton event fluences. *IEEE Transactions on Nuclear Science*, *46*, 1481–1485. <https://doi.org/10.1109/23.819111>
- Xapsos, M. A., Summers, G. P., Barth, J. L., Stassinopoulos, E. G., & Burke, E. A. (2000). Probability model for cumulative solar proton event fluences. *IEEE Transactions on Nuclear Science*, *47*, 486–490. <https://doi.org/10.1109/23.856469>
- Yin, P., Mitchell, C., & Bust, G. (2006). Observations of the F region height redistribution in the storm-time ionosphere over Europe and the USA using GPS imaging. *Geophysical Research Letters*, *33*, L18803. <https://doi.org/10.1029/2006GL027125>
- Zhang, Y., & Paxton, L. J. (2008). An empirical Kp-dependent global auroral model based on TIMED/GUVI FUV data. *Journal of Atmospheric and Solar-Terrestrial Physics*, *70*, 1231–1242. <https://doi.org/10.1016/j.jastp.2008.03.008>
- Ziegler, J. F. (1996). Terrestrial cosmic rays. *IBM Journal of Research and Development*, *40*, 19–39. <https://doi.org/10.1147/rd.401.0019>

### Reference From the Supporting Information

- Cabinet Office. (2012). *National Risk Register 2020* (2012 edition). <https://www.gov.uk/government/publications/national-risk-register-2020>